Dynamics of Nucleus-Nucleus Collisions and Neutron Rearrangement in Time-Dependent Approach

V.V. Samarin, Yu.E. Penionzhkevich, M.A. Naumenko, N.K. Skobelev, Yu.G. Sobolev

FLEROV LABORATORY of NUCLEAR REACTIONS
Joint Institute for Nuclear Research, Dubna, Russia

European Nuclear Physics Conference, Bologna, September 2018

Outline

1. Role of neutron transfer in the dynamics of nucleus-nucleus collisions.
2. Time-dependent analysis of nucleon rearrangement in nucleus-nucleus collisions.
3. Few-neutron transfer reactions with ^{3,6}He nuclei.
4. Neutron rearrangement and total cross sections of reactions with ^{9,11}Li nuclei.
5. Nucleon rearrangement in fusion and multi-nucleon transfer reactions with ^{40}Ca nucleus.

1. Role of nucleon transfer in dynamics of nucleus-nucleus collisions

- Leads to transfer channels (stripping, pickup, multi-nucleon transfer)

- Leads to change in the potential energy of nuclei which
  - changes the cross-section of individual channels (e.g., fusion) and the total reaction cross section compared to the model of nuclei with "frozen" neutrons, which is important in the calculation of the cross sections;
  - may justify the use of phenomenological potentials depending on the energy and the orbital momentum within the optical model (OM), the distorted wave Born approximation (DWBA), etc.

2.1. Theoretical model basics

The microscopic approach based on the numeric solution of the time-dependent Schrödinger equation [1-4] for the outer and inner neutrons and protons of colliding nuclei.

- Classical motion of cores.
- Time-dependent Schrödinger equation (**TDSE**) to describe neutron rearrangement and modification of the barrier of the nucleus-nucleus potential

$$i\hbar\frac{\partial}{\partial t}\Psi(\mathbf{r},t)=\left\{-\frac{\hbar^2}{2m}\Delta+V_1\left(\left|\mathbf{r}-\mathbf{r}_1(t)\right|\right)+V_2\left(\left|\mathbf{r}-\mathbf{r}_2(t)\right|\right)+\hat{V}_{LS}^{(1)}(\mathbf{r}-\mathbf{r}_1(t))+\hat{V}_{LS}^{(2)}(\mathbf{r}-\mathbf{r}_2(t))\right\}\Psi(\mathbf{r},t), \qquad \Psi(\mathbf{r},t)=\begin{pmatrix}\psi(\mathbf{r},t)\\ \phi(\mathbf{r},t)\end{pmatrix}$$

- The initial wave functions were determined from the spherical shell model with parameters providing reasonable values of charge radius and separation energies of outer neutrons and protons.
- The initial conditions for the proton wave functions included the long-range character of the Coulomb interaction with the other nucleus. For instance, the proton wave function in the isolated projectile nucleus at a finite distance from the target nucleus was preliminarily subjected to slow (adiabatic) switching of the Coulomb interaction with the target nucleus. Thus, the polarization effects of the proton cloud were already taken into account in the initial condition.

[1] V. Samarin. Phys. Atom. Nucl. **78**, 128 (2015).
[2] V. Samarin, EPJ Web Conf. **66**, 03075 (2014).
[3] V. Samarin, EPJ Web Conf. **86**, 00040 (2015).
[4] V. Samarin et al. Bull. Russ. Acad. Sci: Phys., **82**, 637 (2018)

Light quantum particle (nucleon) 3

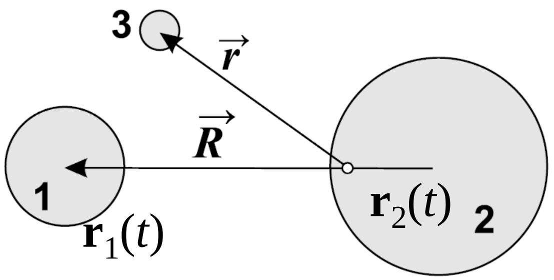

Two heavy classical particles (cores) 1 and 2

2.2. Benefits of time-dependent Schrödinger equation approach

- **quantum description of several independent external neutrons,**
- **small 3D mesh step (0.1 - 0.2 fm, smaller than the length of the probability density oscillations),**
- **classical description of motion of centers of nuclei,**
- **may be used for both light and heavy nuclei,**
- **fast calculation,**
- **intuitive visualization of dynamics.**

3.1. Calculation of probability and cross section for neutron pickup in reaction ^{3}He+ ^{45}Sc

Neutron pickup probability

$$p_1(b,E) = \lim_{t\to\infty} W_1(b,E,t)$$

W_1 is integral of probability density in vicinity of projectile nucleus (~3 fm)

Pickup cross section

$$\sigma(E) = \int_0^\infty p_1(b,E)\,b\,db$$

b is impact parameter

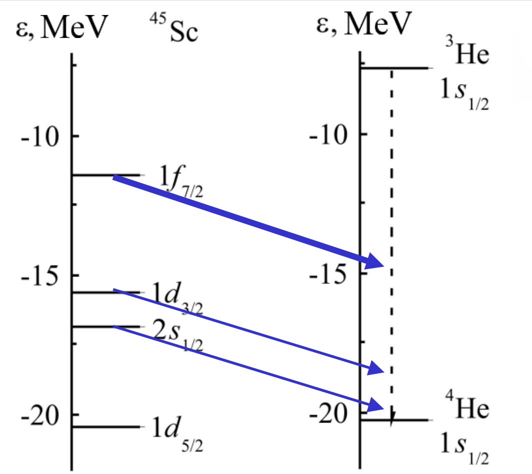

Scheme of neutron levels of nuclei ^{45}Sc and ^{3}He in model of pickup reaction.

$$p(b,E) \approx \exp\left[A(E) - B(E)R_{\min}(b,E)\right]$$

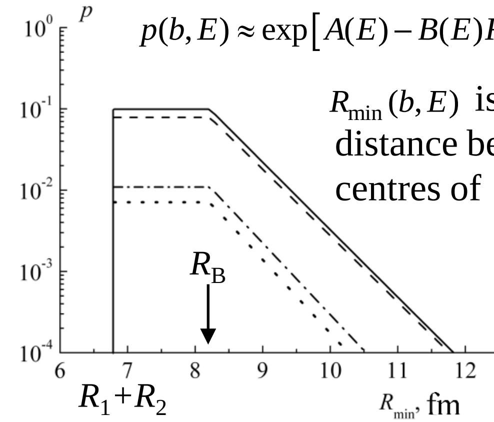

$R_{\min}(b,E)$ is minimum distance between centres of nuclei

Total pickup probability for neutron from nucleus ^{45}Sc (solid line) and pickup probabilities from states $1f_{7/2}$ (dashed line), $2s$ (dash-dotted line), and $1d_{3/2}$ (dotted line) at energy E_{cm} = 15 MeV.

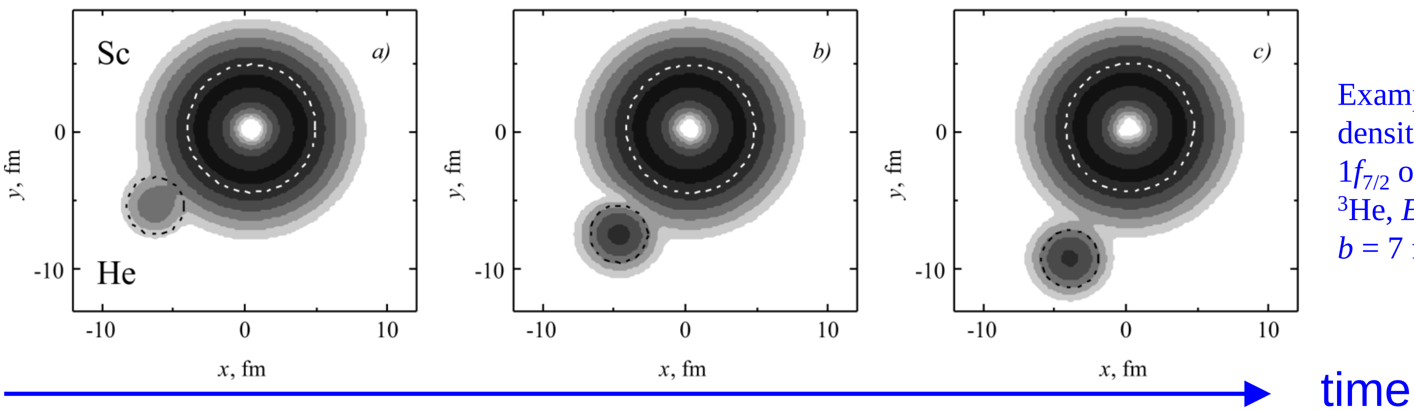

Example of evolution of probability density for pickup of external neutron $1f_{7/2}$ of nucleus ^{45}Sc in collision with ^{3}He, E_{cm} = 8 MeV, impact parameter b = 7 fm.

^{3}He including only 1 neutron in field of heavier core, makes it possible to study transfer process in simplest case

3.2. Calculation of probability and cross section for neutron stripping in reaction ^{3}He+ ^{45}Sc

Neutron stripping probability

$$\bar{p}_2(b,E) = \lim_{t\to\infty} \sum_k |a_k(t)|^2$$

a_κ are occupations of initially free levels (above Fermi level) in target (integral would include occupations of all levels)

Stripping cross section

$$\sigma(E) = \int_0^\infty \bar{p}_2(b,E)\, b\, db$$

b is impact parameter

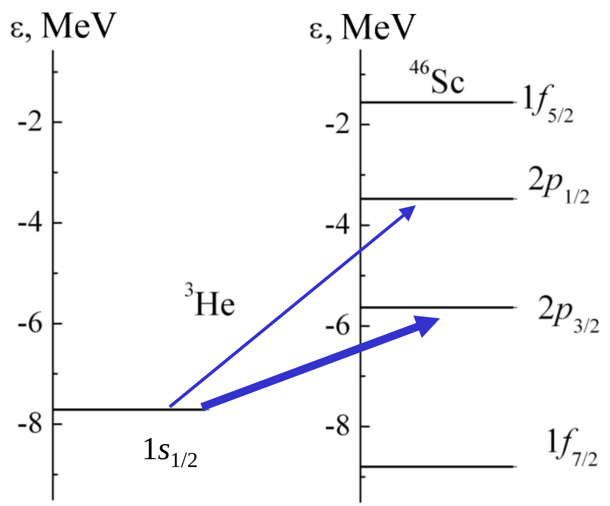

Scheme of neutron levels of nuclei ^{3}He and ^{46}Sc in model of stripping reaction.

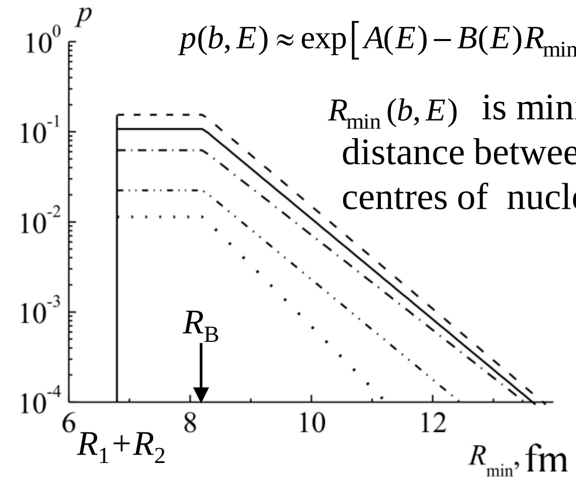

$$p(b,E) \approx \exp\left[A(E) - B(E) R_{min}(b,E)\right]$$

$R_{min}(b,E)$ is minimum distance between centres of nuclei

Neutron stripping probability to states $2p_{3/2}$ and $2p_{1/2}$ (dash-dotted), $1f_{5/2}$ (dash-dot-dotted), $1f_{7/2}$ (dotted) at energy E_{cm} = 15 MeV.

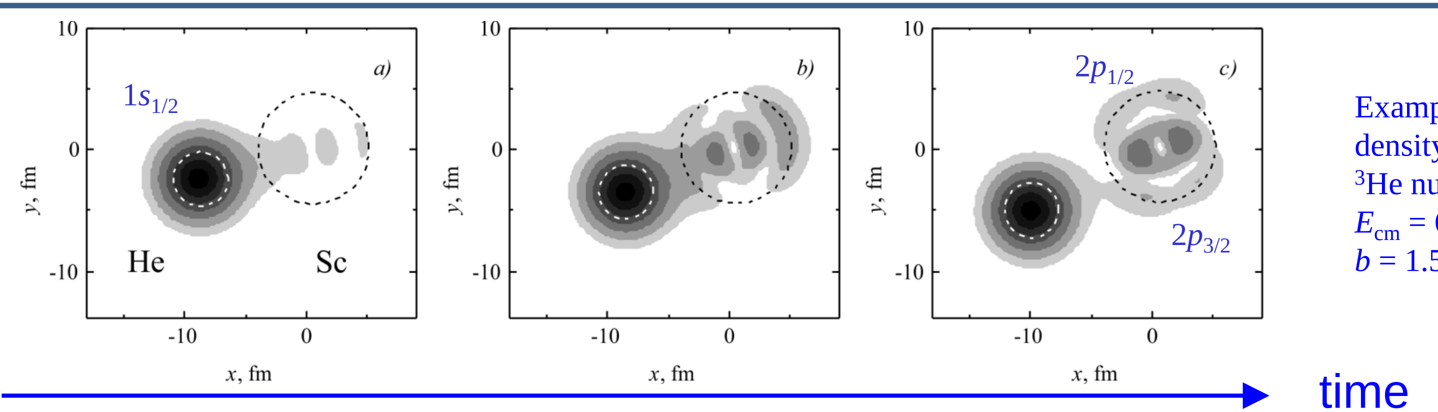

Example of evolution of probability density for stripping of neutron of ^{3}He nucleus in collision with ^{45}Sc, E_{cm} = 6.5 MeV, impact parameter b = 1.5 fm.

^{3}He including only 1 neutron in field of heavier core, makes it possible to study transfer process in simplest case

3.3. Calculation of cross sections for formation of isotopes ^{44}Sc and ^{46}Sc in reaction ^{3}He + ^{45}Sc

$$\sigma_{\mathrm{tr}}(E) = \int_0^{\infty} p(b,E)\, b\, db$$

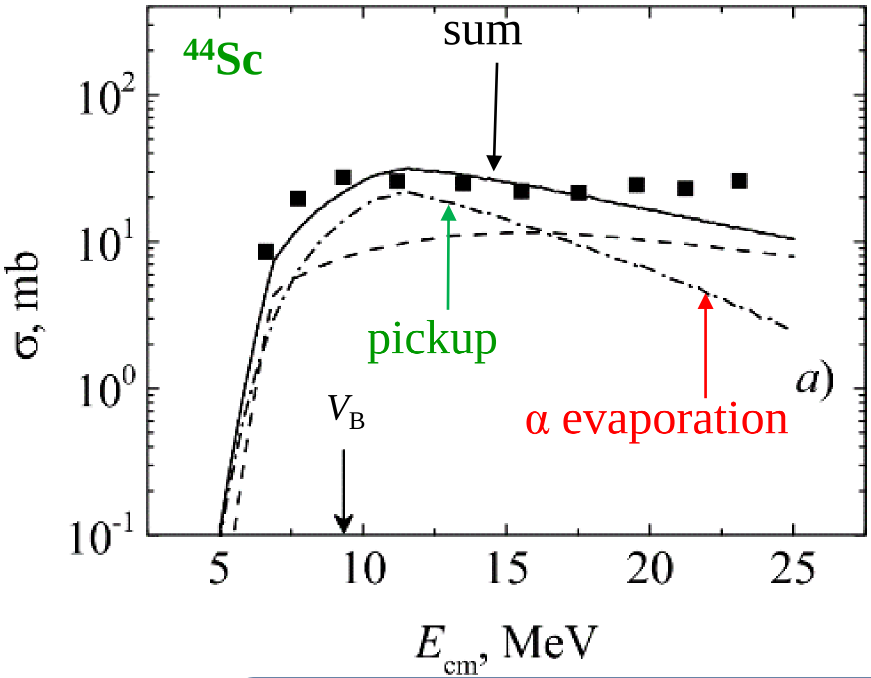

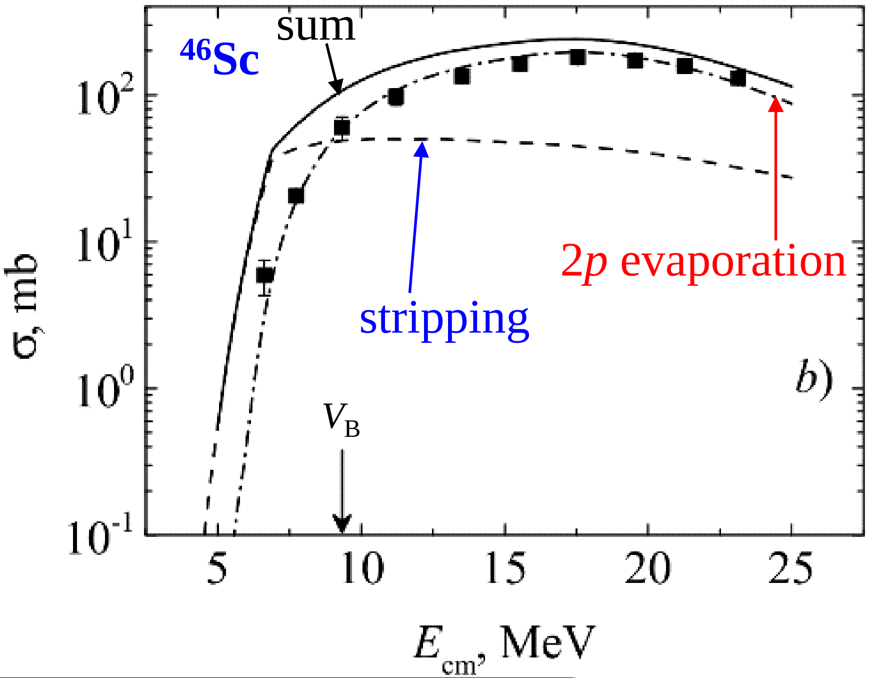

Good agreement with experimental data.
Pickup cross section is lower than stripping cross section.
Contribution of fusion-evaporation is high.

[1] (Experiment) N. K. Skobelev, A. A. Kulko, Yu. E. Penionzhkevich et al. Phys. Part. Nucl. Lett. 2013. V. 10. P. 410.
[2] (Evaporation code) NRV web knowledge base on low-energy nuclear physics. URL: http://nrv.jinr.ru/

3.4. Results of calculation of cross section for formation of isotope ^{45}Ti in reaction ^{3}He + ^{45}Sc

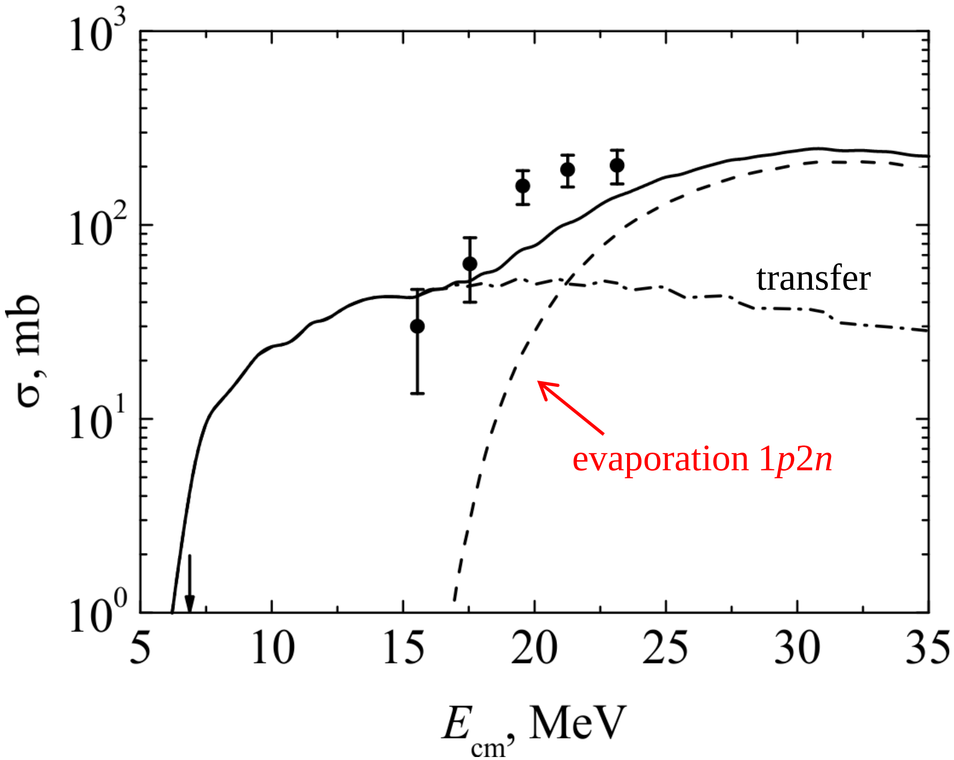

$$\sigma(E) = \int_0^\infty \left[P_1(b,E) + P_2(b,E) \right] b\,db$$

Transfer mechanisms

First mechanism of ^{45}Sc formation with probability P_1:
a) proton transfer to quasi-stationary excited states lower than sum of Coulomb and centrifugal barriers for protons;
b) proton transition to lower bound states with neutron emission.

Second mechanism of ^{45}Sc formation with probability P_2:
a) proton transfer (stripping) from projectile to target;
b) neutron transfer (pickup) from target to projectile.

Fusion-evaporation mechanism

Third mechanism of ^{45}Sc formation
a) fusion with formation of compound nucleus;
b) evaporation of one proton and two neutrons.

Good agreement with experimental data.
Contribution of fusion-evaporation is significant.

Correlated proton stripping and neutron pickup mechanism is proposed for description of reaction ^{45}Sc (^{3}He, ^{3}H) ^{45}Ti

[1] (Experiment) N. K. Skobelev, A. A. Kulko, Yu. E. Penionzhkevich et al. Phys. Part. Nucl. Lett. 2013. V. 10. P. 410.
[2] (Evaporation code) NRV web knowledge base on low-energy nuclear physics. URL: http://nrv.jinr.ru/

3.5. Neutron stripping in reaction $^{3}He + ^{197}Au$

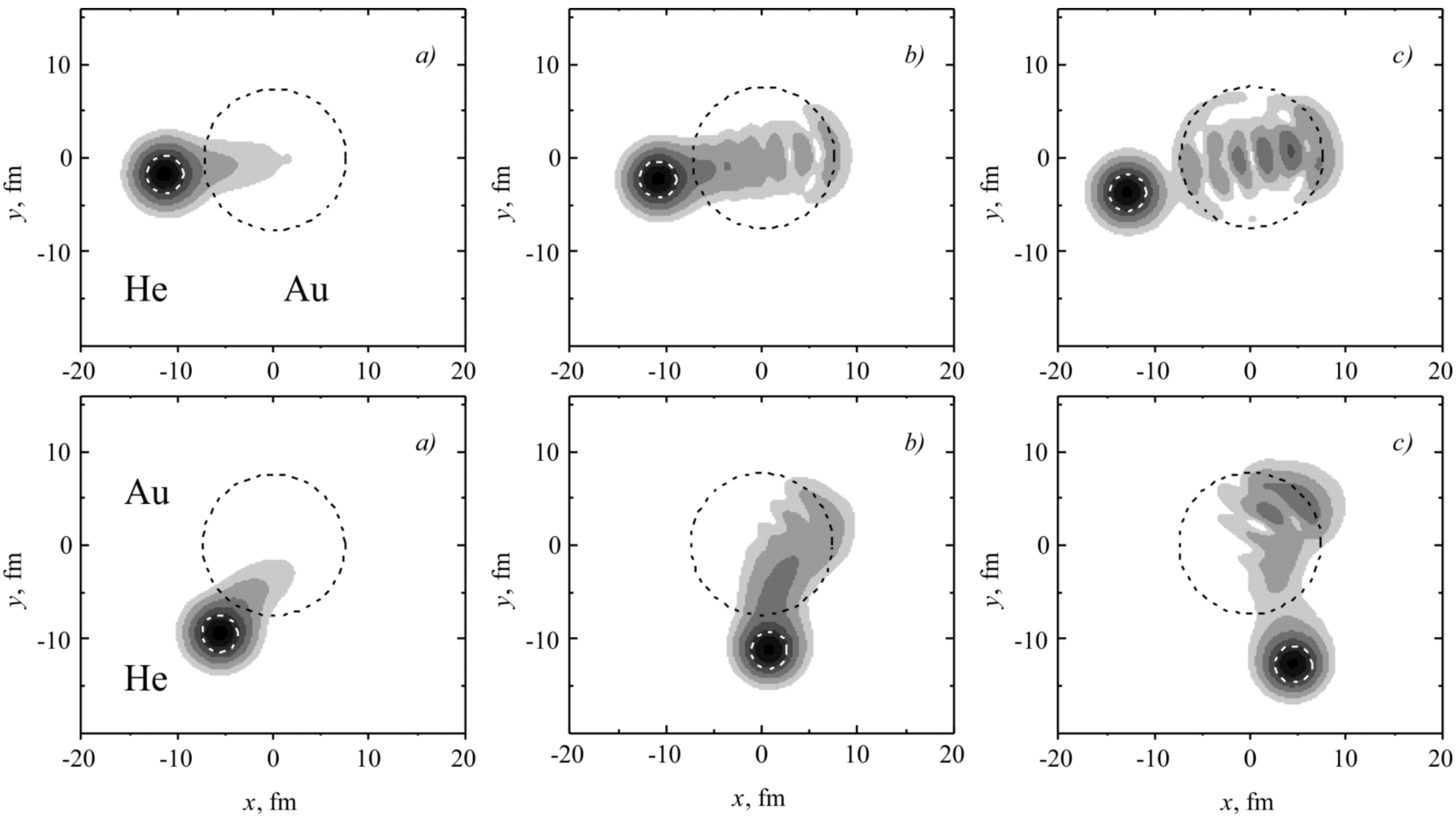

Example of time evolution of the probability density for the neutron of ^{3}He in the collision with ^{197}Au at E_{cm} = 20 MeV, impact parameter b =1 fm (a-c) and at E_{cm} = 40 MeV, b =7.5 fm (e-g). Radii of circumferences equal the effective radii of nuclei R_1 = 2 fm, R_2 = 7.5 fm. The course of time corresponds to the panel locations (a,b,c) and (e,f,g).

3.6. Calculation of cross sections for formation of isotopes ^{196}Au and ^{198}Au in reaction ^{3}He + ^{197}Au

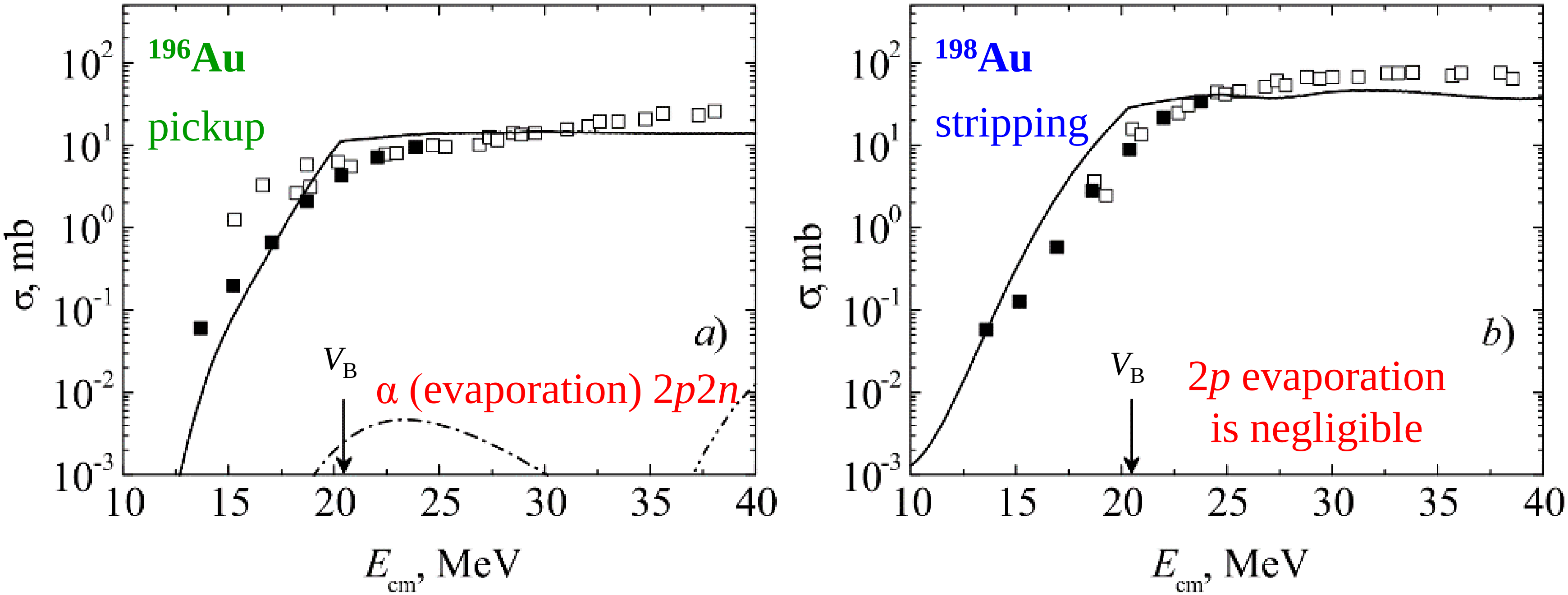

Good agreement with experimental data.
Pickup cross section is lower than stripping cross section.
Contribution of fusion-evaporation is negligible.

[1] (Experiment ■) N. K. Skobelev, Yu. E. Penionzhkevich, E. I. Voskoboynik et al. Phys. Part. Nucl. Lett. 2014. V. 11. P. 114.
[2] (Experiment □) Y. Nagame, K. Sueki, S. Baba, and H. Nakahara. Phys. Rev. C. 1990. V. 41. P. 889.
[3] (Evaporation code) NRV web knowledge base on low-energy nuclear physics. URL: http://nrv.jinr.ru/

3.7. Evolution of proton probability density for collision $^{3}He + ^{194}Pt$: proton stripping

Excited quasi-stationary states lower than sum of Coulomb and centrifugal barriers for protons

neutron emission

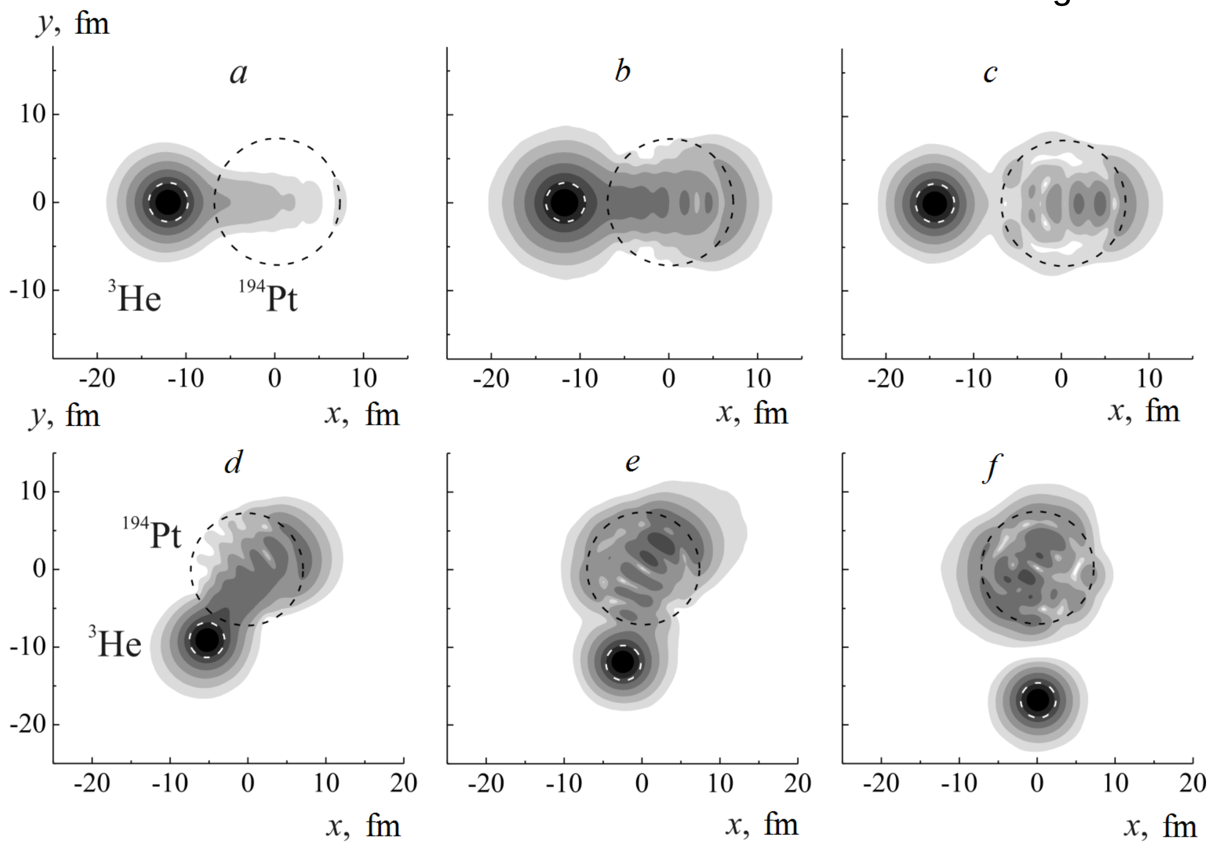

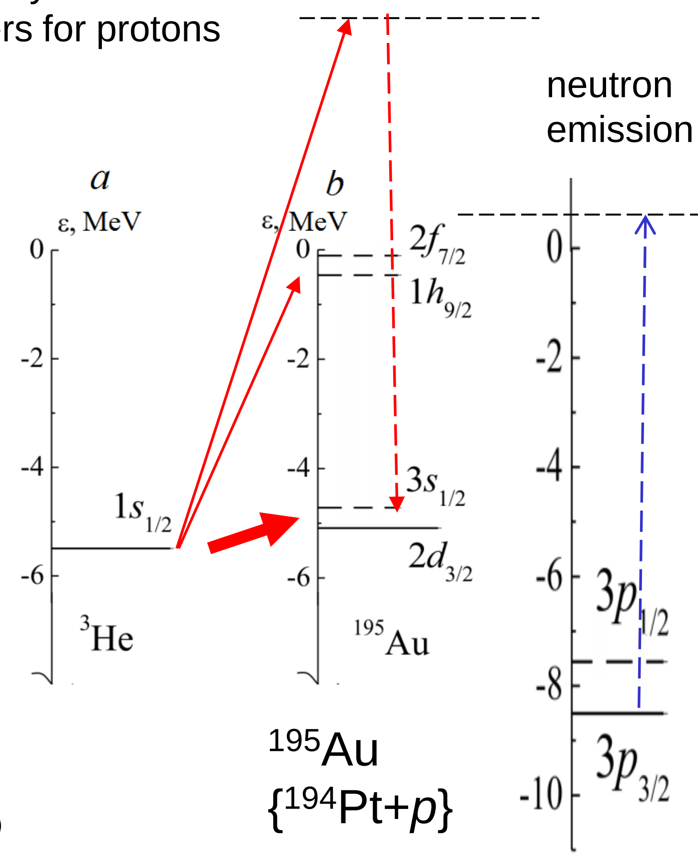

^{195}Au $\{^{194}Pt+p\}$

^{194}Pt

time

a-b-c: E_{cm}= 19 MeV, b = 0

d-e-f: E_{cm}= 25 MeV, b = 4.6 fm

First mechanism of ^{194}Au formation with probability P_1

3.8. Results of calculation of cross section for formation of isotope ^{194}Au in reaction ^{3}He + ^{194}Pt

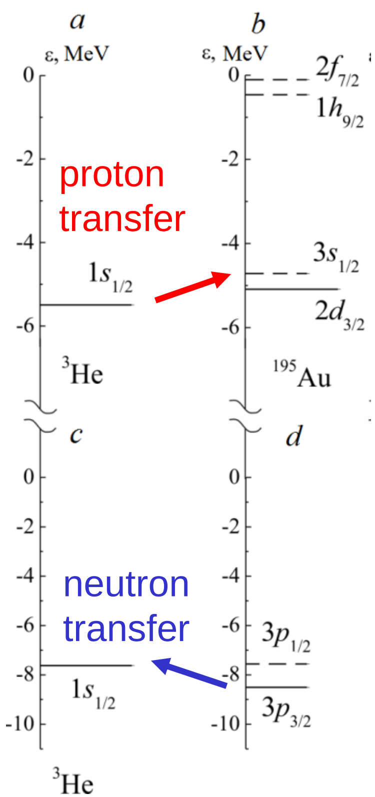

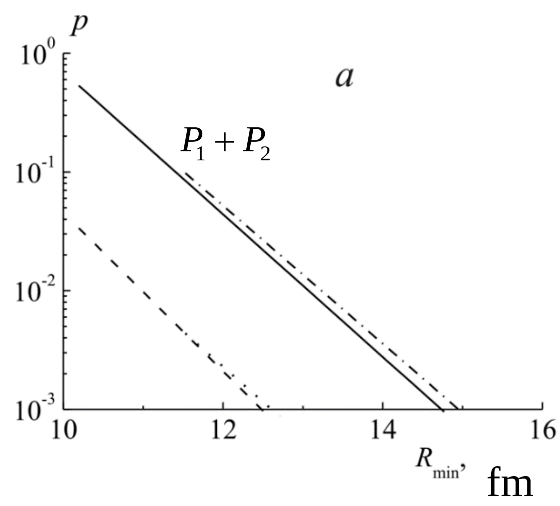

$$\lg P_{1,2}(b,E) \approx A_{1,2}(E) - B_{1,2}(E) R_{\min}(b,E)$$

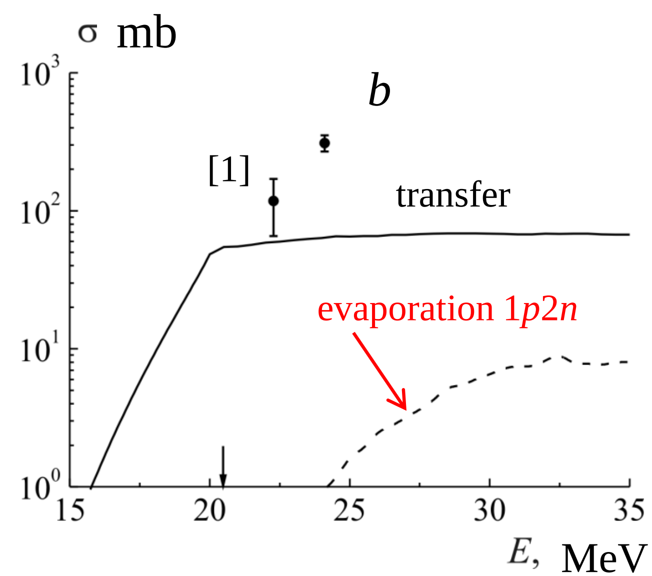

$$\sigma(E) = \int_0^{\infty} \left[P_1(b,E) + P_2(b,E) \right] b\,db$$

Second mechanism of ^{194}Au formation with probability P_2: resonance tunneling to levels with close energies

(a) Total probability P_1+P_2 of proton transfer from ^{3}He to ^{194}Pt as a function of distance $R_{\min}$ of minimum approach for E_{cm} = 25 MeV (solid line), 19 MeV (dashed-and-dotted line) and probability of transfer to discrete spectrum states with energies above Fermi level for E_{cm} = 25 MeV (dashed line) and 19 MeV (dotted line). (b) Cross section for formation of ^{194}Au in ^{3}He + ^{194}Pt reaction. Dots are experimental data from [1], solid line is estimated contribution from neutron evaporation after proton transfer. Dashed line shows contribution of the fusion-evaporation mechanism calculated using code of NRV knowledge base [2].

[1] (Experiment) Skobelev, N.K. et al., Phys. Part. Nucl. Lett., 2014, vol. 11, p. 114.
[2] (Evaporation code) NRV web knowledge base on low-energy nuclear physics. URL: http://nrv.jinr.ru/

3.9. Calculation of probability and cross section for neutron stripping in reaction ^{6}He + ^{197}Au

Neutron stripping probability

$$\bar{p}_2(b,E) = \lim_{t\to\infty} \sum_k |a_k(t)|^2$$

a_κ are occupations of initially free levels (above Fermi level) in target (integral would include occupations of all levels)

Stripping cross section

$$\sigma(E) = \int_0^\infty \bar{p}_2(b,E)\, b\, db$$

b is impact parameter

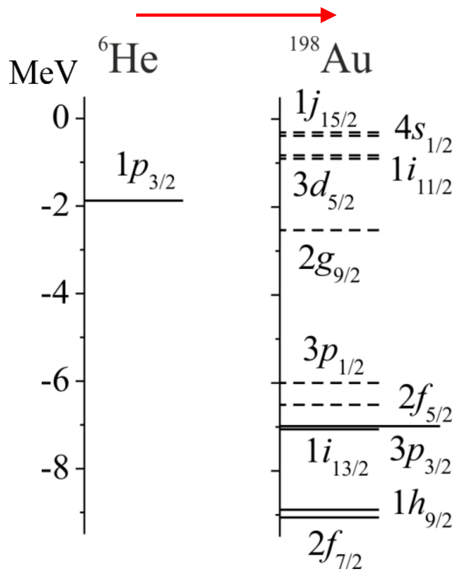

Scheme of neutron levels of nuclei ^{6}He and ^{198}Au in model of stripping reaction.

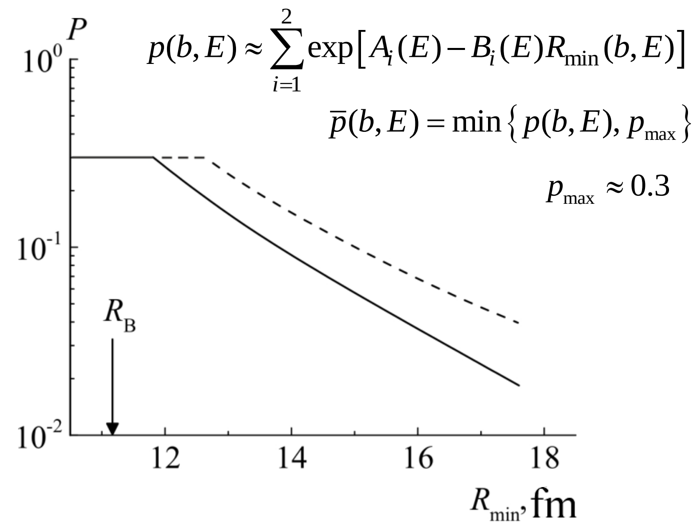

Dependence of neutron stripping probability on distance R_{min} of minimum approach for neutron transfer from ^{6}He to ^{197}Au (E_{cm} = 19 MeV and 25 MeV, dashed and solid curves, respectively).

$R_{\min}(b,E)$ is minimum distance between centres of nuclei

Based on results for ^{3}He, more complicated case of ^{6}He (2 neutrons, halo) is analyzed

3.10. Animation: Evolution of neutron probability density for collision $^{6}He + ^{197}Au$: neutron stripping from ^{6}He and breakup

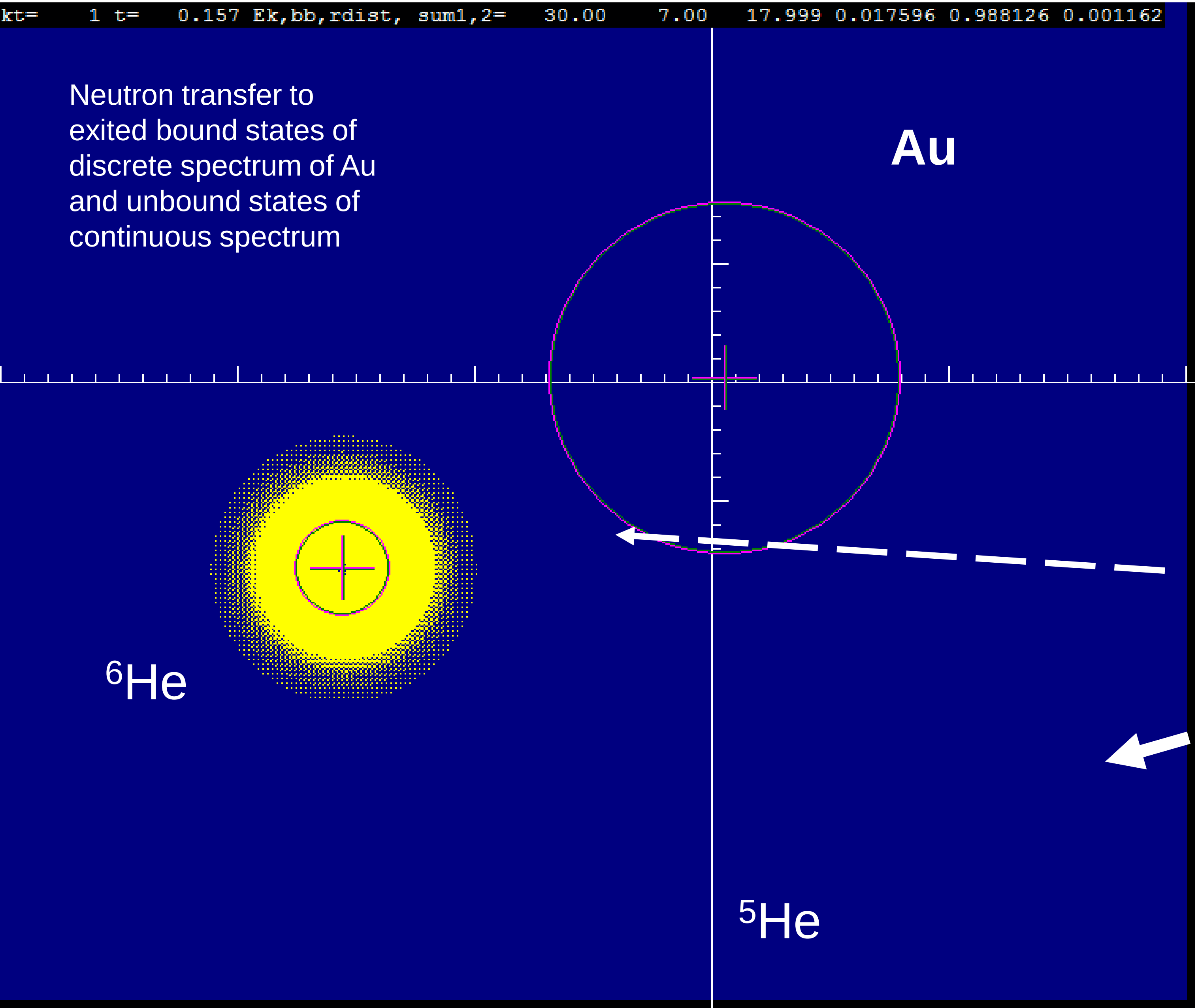

Evolution of probability density for valence neutron of ^{6}He in collision $^{6}He + ^{197}Au$ in model with

$E(1p_{3/2}) = -E_{sep}(1n) =$

$= -1.8$ MeV,

$E_{cm} = 30$ MeV $> V_B$.

Potential well of ^{6}He is transformed into well of ^{5}He after neutron transfer from He to Au.

Breakup of ^{5}He after neutron transfer to Au.

^{6}He (2 neutrons, halo) is more complicated case compared with ^{3}He

3.11. Animation: Evolution of neutron probability density for collision ^{6}He + ^{197}Au: neutron pickup to metastable states of He

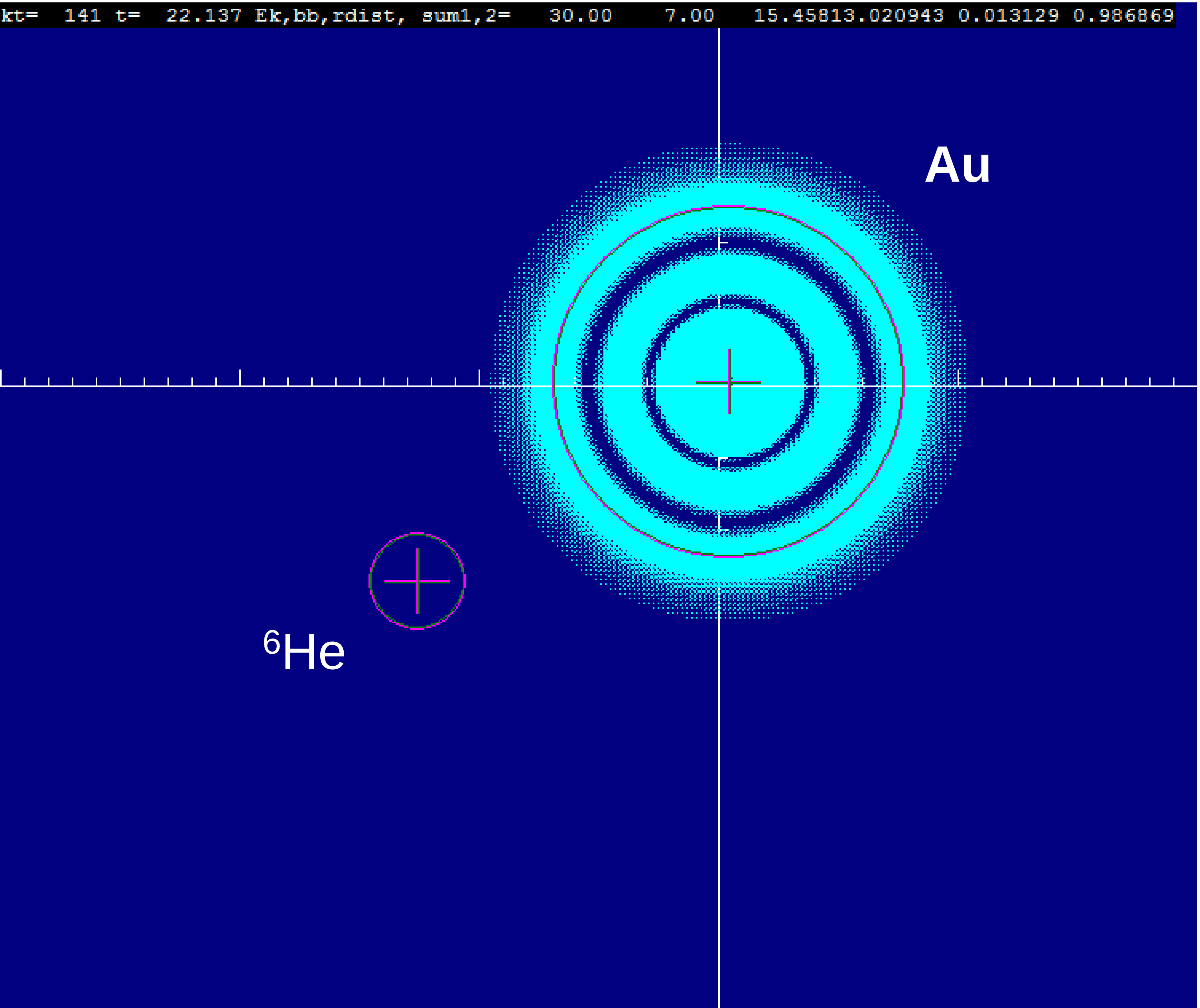

Evolution of probability density for neutron of ^{197}Au from level $3p_{3/2}$ in collision ^{6}He + ^{197}Au at E_{cm} = 30 MeV > V_B.

Formation of ^{196}Au by:
first mechanism – collision of α-core of ^{6}He with neutrons in periferical region of Au in grasing collision ^{6}He+Au;
Second mechanism – neutron transfer from Au to He.

Breakup of ^{7}He after neutron transfer to He.

3.12. Calculation of cross sections for formation of isotopes ^{196}Au and ^{198}Au in reaction ^{6}He + ^{197}Au

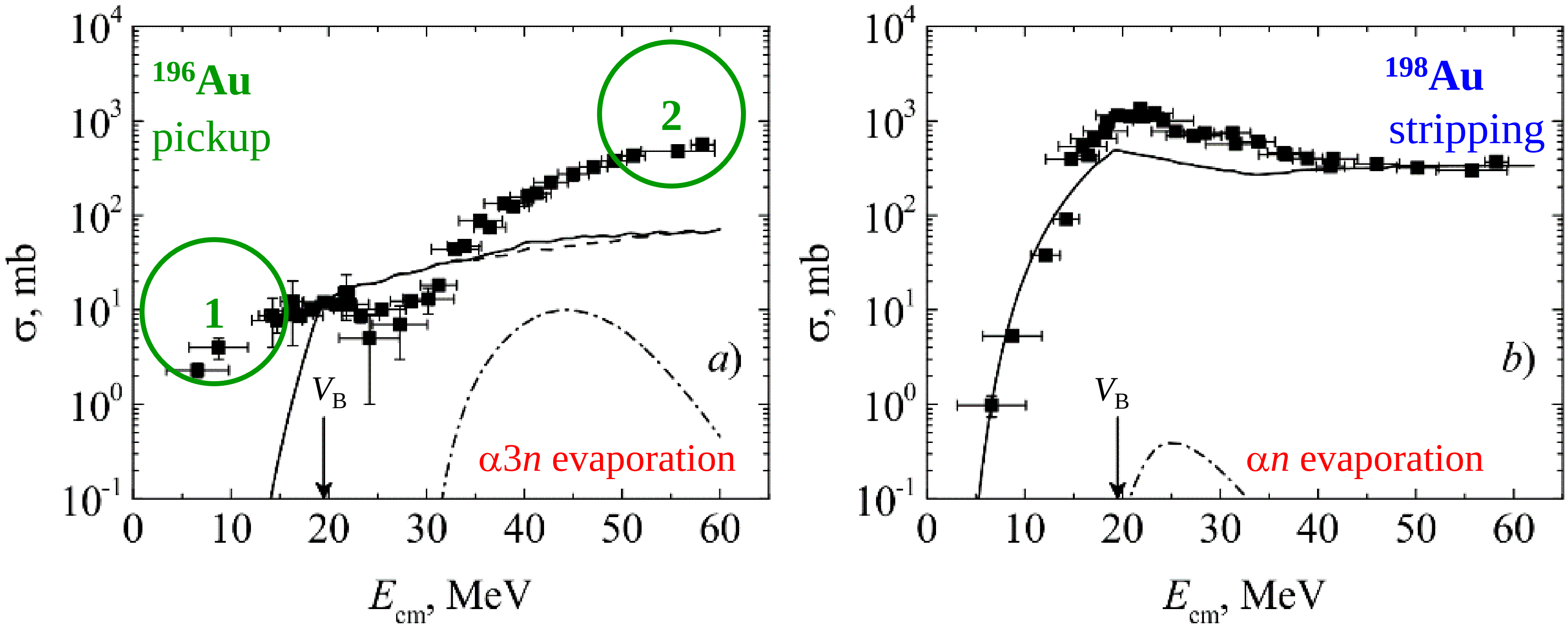

Reasonable agreement with experimental data.
Contribution of fusion-evaporation is low.
Calculated pickup cross section is lower than calculated stripping cross section.
Experimental points in regions 1 and 2 of ^{196}Au data may be results of contributions of other channels.

[1] (Experiment) Yu. E. Penionzhkevich, R. A. Astabatyan, N. A. Demekhina et al. Eur. Phys. J. A. 2007. V. 31. P. 185.
[2] (Evaporation code) NRV web knowledge base on low-energy nuclear physics. URL: http://nrv.jinr.ru/

3.13. Calculation of cross sections for formation of isotopes ^{46}Sc in reaction ^{6}He + ^{45}Sc and ^{65}Zn in reaction ^{6}He + ^{64}Zn

[1]

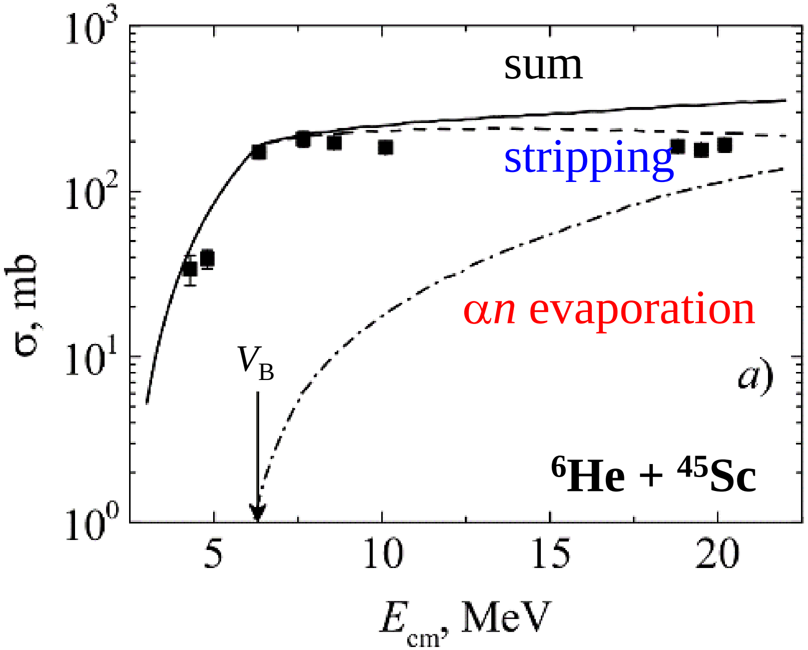

[2]

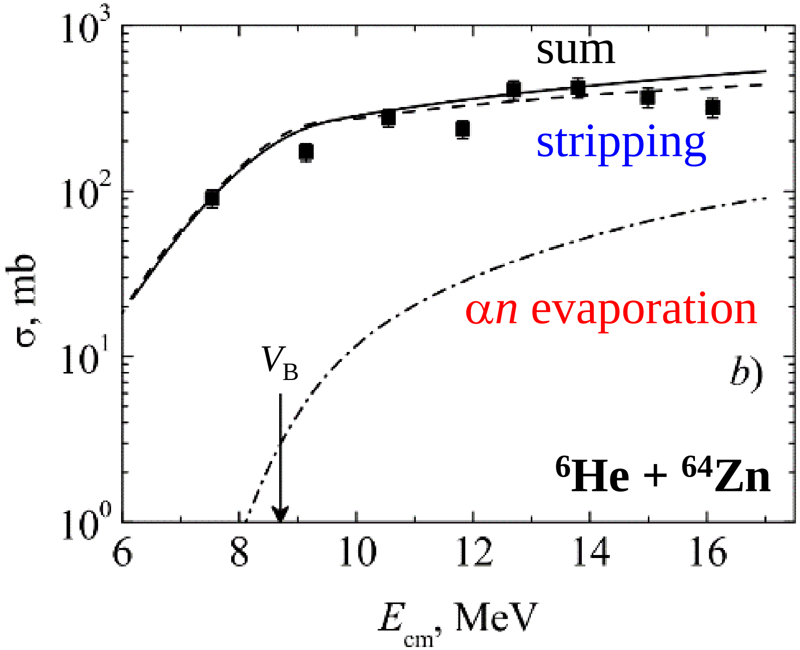

Good agreement with experimental data.
Contribution of fusion-evaporation is noticeable.

[1] (Experiment with ^{45}Sc) N. K. Skobelev, A. A. Kulko, V. Kroha et al. J. Phys. G: Nucl. Part. Phys. 2011. V. 38. P. 035106.
[2] (Experiment with ^{64}Zn) V. Scuderi, A. Di Pietro, P. Figuera et al. Phys. Rev. C. 2011. V. 84. P. 064604.
[3] (Evaporation code) NRV web knowledge base on low-energy nuclear physics. URL: http://nrv.jinr.ru/

4.1. Experimental data on total cross sections of reactions with $^{9,11}Li$ nuclei

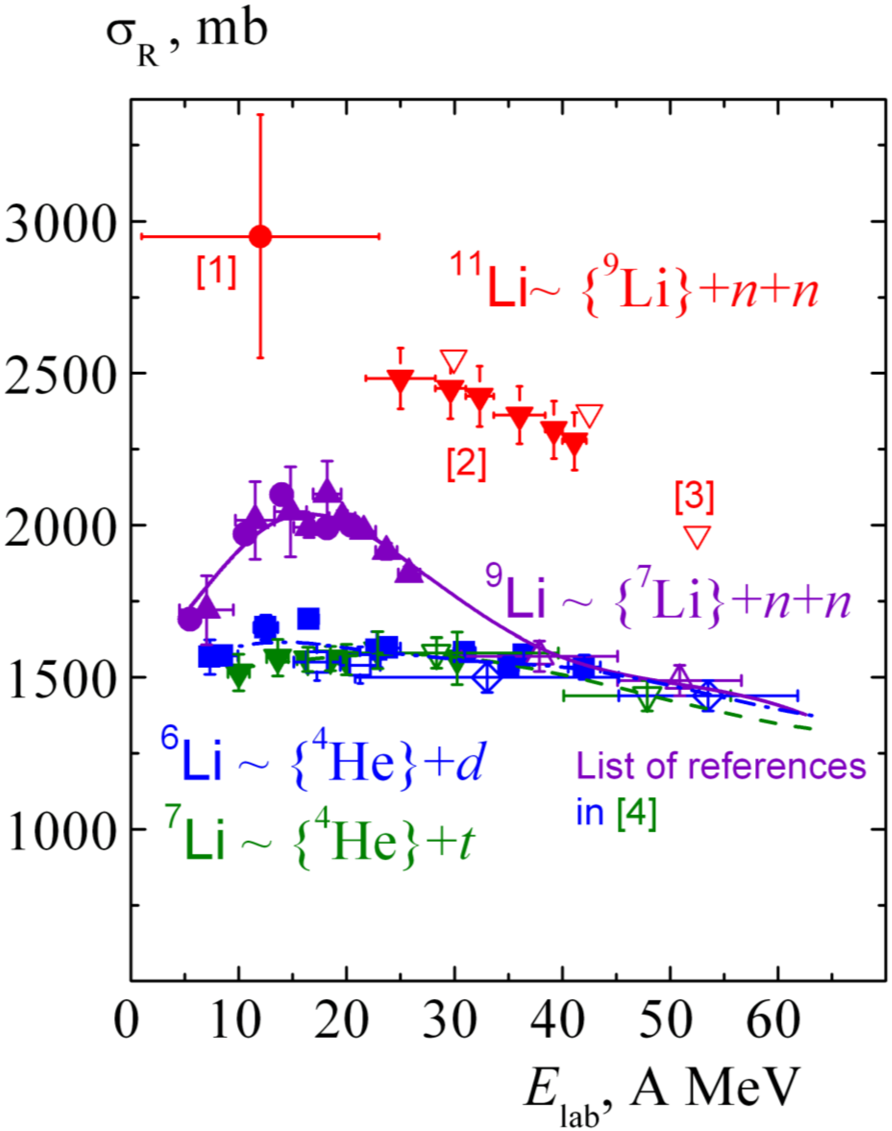

A series of experiments on measurement of total cross sections for reactions $^{6,7,9,11}Li$ + ^{28}Si in the beam energy range 5–50 A MeV was performed at Flerov Laboratory of Nuclear Reactions (FLNR), Joint Institute for Nuclear Research (JINR) and some other laboratories. The interesting results were the unusual enhancements of total cross sections for $^{9,11}Li$ + ^{28}Si reactions as compared with $^{6,7}Li$ + ^{28}Si reactions.

[1] A.C. Villari *et al.,* Phys. Lett. B **268**, 345 (1991).

[2] Li Chen *et al.,* High Energy Physics and Nuclear Physics **31**, 1102 (2007).

[3] R.E. Warner *et al*., Phys. Rev. C **54**, 1700 (1996).

[4] Yu. E. Penionzhkevich *et al*., Phys. Atom. Nucl., **80**, 928 (2017).

4.2. Animation: Evolution of neutron probability density for collision $^{9}Li+^{28}Si$

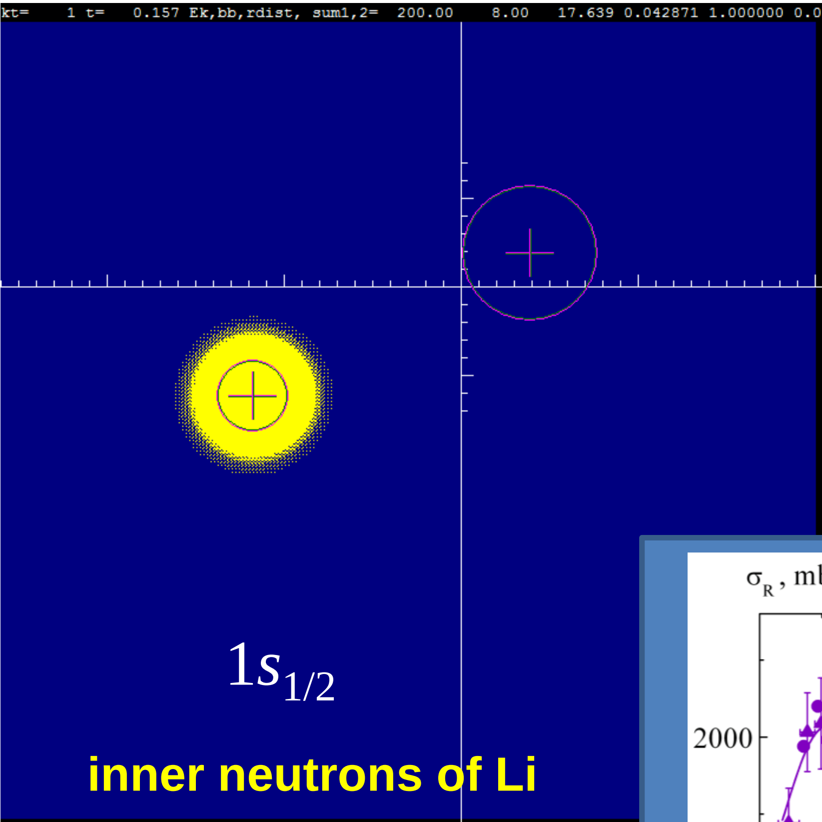

E_{lab}= 30 A MeV

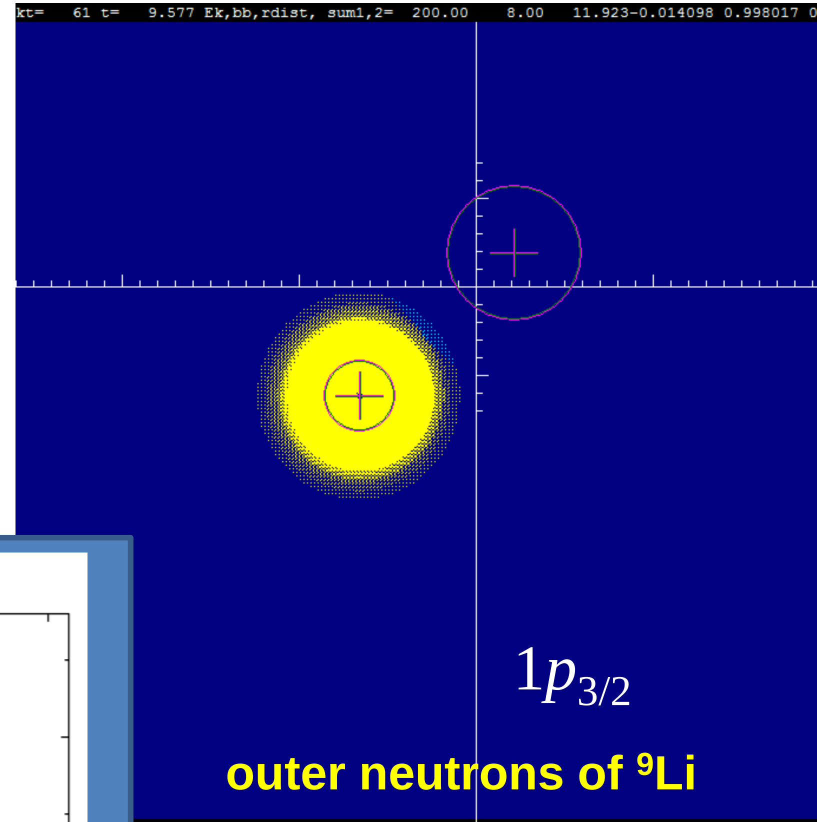

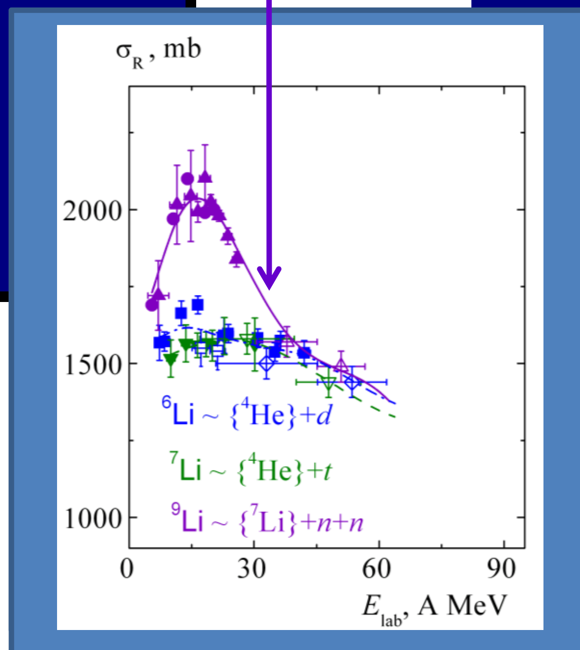

Time evolution of probability density $|\Psi|^2$ for strongly bound neutrons is similar to the motion of the “frozen” shell.

Time evolution of probability density $|\Psi|^2$ for weakly bound neutrons: appreciable rearrangement of neutrons between nuclei.

4.3. A physical mechanism is proposed that explains the presence of a sharp maximum in the total cross section of the $^{9}Li + ^{28}Si$ reaction in the energy range 10−20 *A* MeV based on the solution of the time-dependent Schrödinger equation for outer neutrons of projectile nuclei

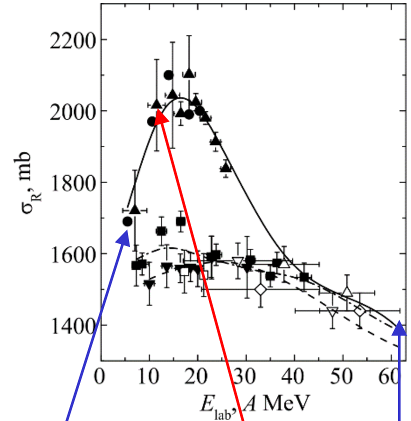

^{9}Li was represented as core $^{7}Li + n + n$

Evolution of the probability density of each of the two outer neutrons of ^{9}Li in collision $^{9}Li + ^{28}Si$:

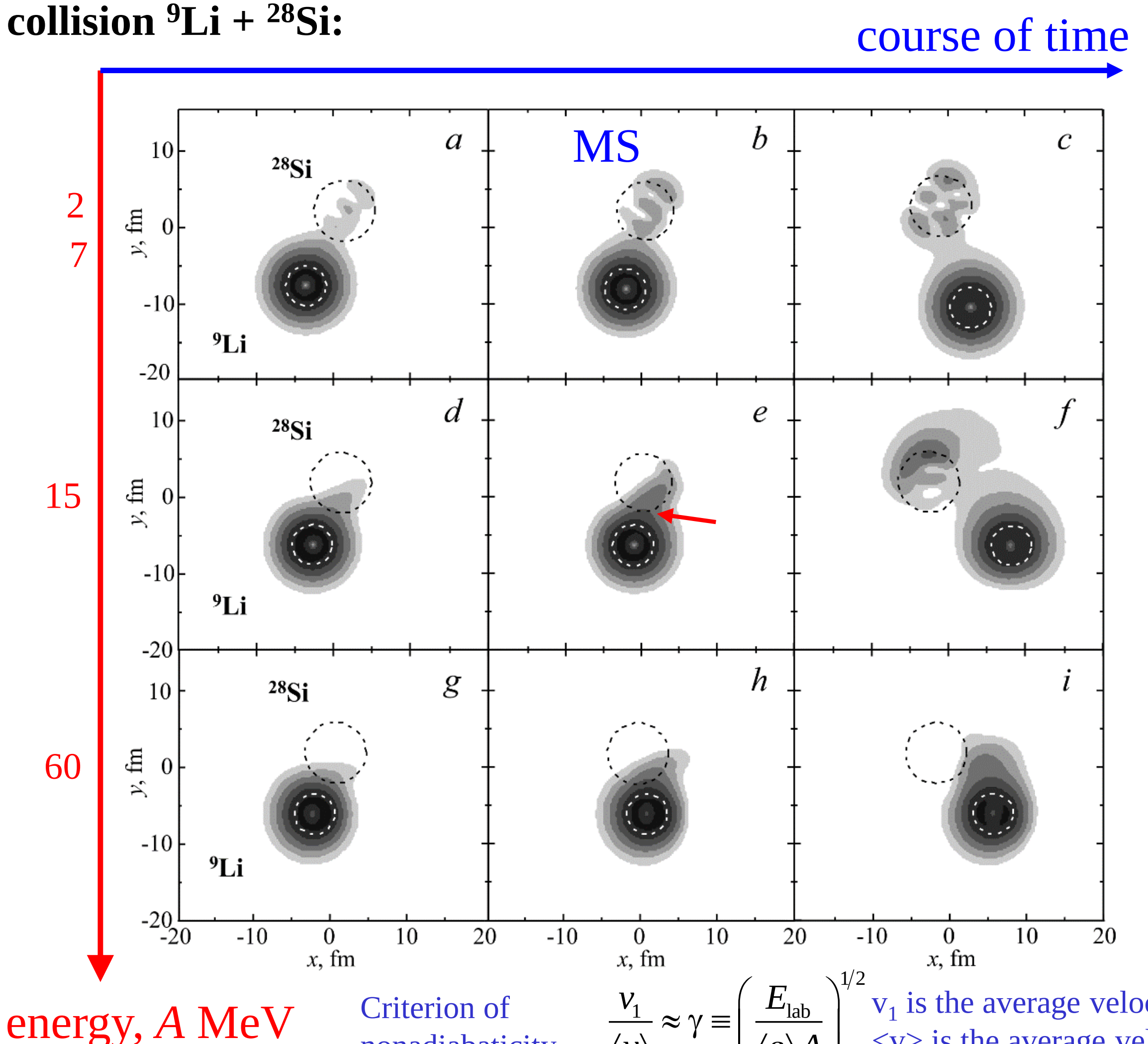

Adiabatic motion:
when the nuclei approach, two-center "molecular" states (MS) are formed;
$v_1 \ll \langle v \rangle$, E_{lab} = 7 *A* MeV

Intermediate case:
a noticeable rearrangement of neutrons in the region between the surfaces of the nuclei;
$v_1 \sim \langle v \rangle$, E_{lab} = 15 *A* MeV

Non-adiabatic motion:
during the collision neutrons do not have time to rearrange;
$v_1 \gg \langle v \rangle$, E_{lab} = 60 *A* MeV

Criterion of nonadiabaticity

$$\frac{v_1}{\langle v \rangle} \approx \gamma \equiv \left(\frac{E_{lab}}{\langle \varepsilon \rangle A} \right)^{1/2}$$

v_1 is the average velocity of the projectile nucleus relative to the target nucleus,
$\langle v \rangle$ is the average velocity of the outer neutron in the projectile nucleus

4.4. Angular distributions for elastic scattering of ^{6,7}Li+^{28}Si and energy-independent nuclear part of nucleus-nucleus optical potential $V + iW$

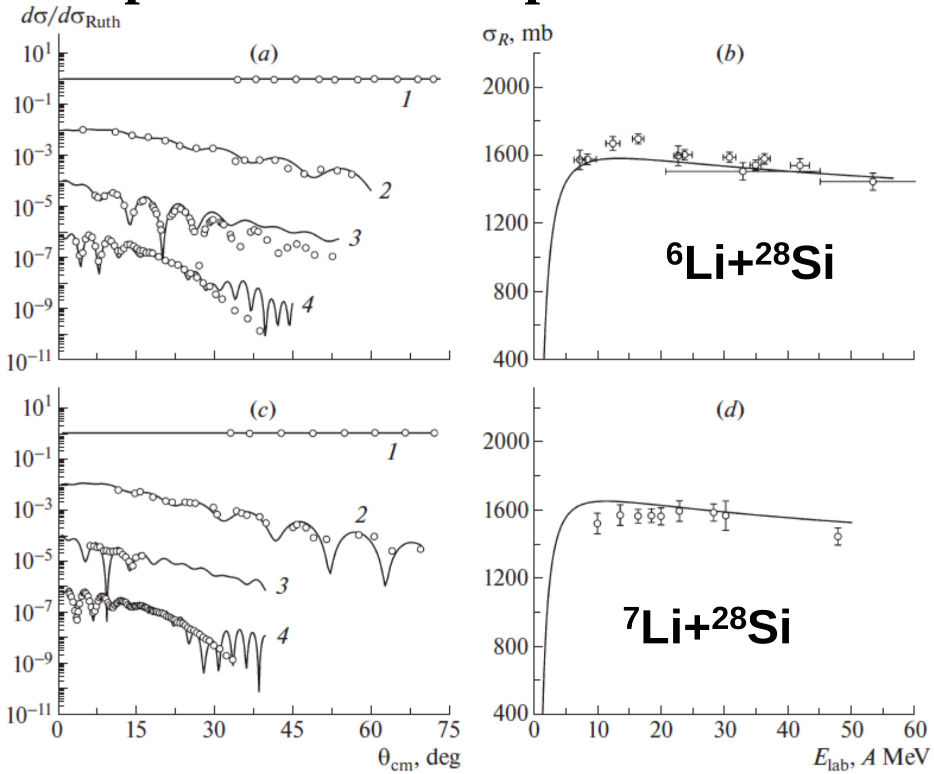

The outer neutrons in ^{6}Li and ^{7}Li are bound into the positively charged deuteron and triton clusters.

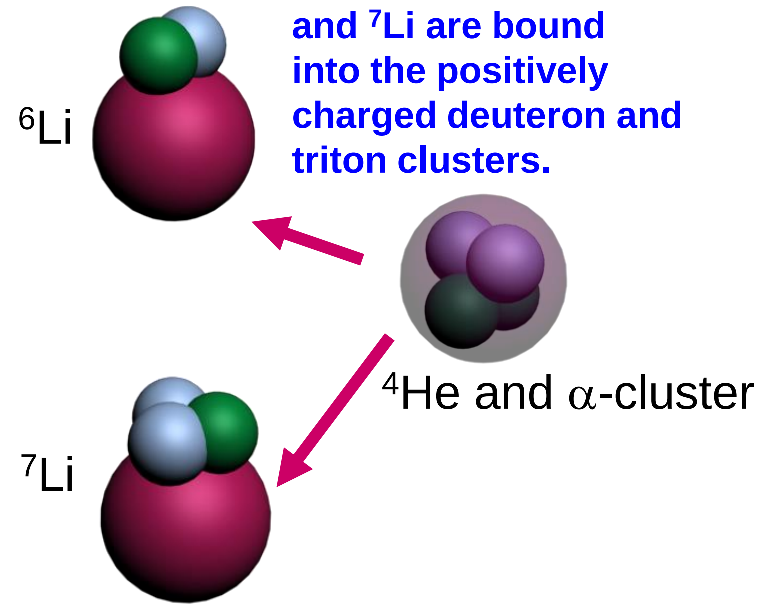

Fig. 4. Experimental angular distributions (points) and results of respective calculations based on the NRV optical model [17] (curves) for the elastic scattering of the following nuclei on ^{28}Si nuclei: (a) ^{6}Li nuclei of energy $E_{lab} = 318$ MeV [18] (curve 4, multiplied by 10^{-6}), 99 MeV [19] (curve 3, multiplied by 10^{-4}), 32 MeV [20] (curve 2, multiplied by 10^{-2}), and 7.5 MeV [21] (curve 1) and (c) ^{7}Li nuclei of energy $E_{lab} = 350$ MeV [22] (curve 4, multiplied by 10^{-6}), 178 MeV [23] (curve 3, multiplied by 10^{-4}), 36 MeV [24] (curve 2, multiplied by 10^{-2}) and 8 MeV [25] (curve 1). Figures 4b and 4d give the total cross sections for, respectively, the ^{6}Li+^{28}Si reactions and the ^{7}Li+^{28}Si reaction. The displayed points stand for experimental data from [2, 3, 9], while the curves represent the results of optical-model calculations.

V. Samarin *et al.*, **Study of Few-Body Nuclei by Feynman's Continual Integrals and Hyperspherical Functions. ENPC-2018 report**

Table 3. Parameters of the optical potential for elastic ^{6,7,9}Li+^{28}Si scattering (the values of the Akyuz–Winther parameters [27])

Reaction	E_{lab}, MeV	r_{0C}, fm	V_0, MeV	r_{0V}, fm	a_V, fm	W_0, MeV	r_{0W}, fm	a_W, fm
^{6}Li+^{28}Si	7.5–318	1.3	19.75 (36.64)	1.245	0.63 (0.583)	120.493	0.948	0.632
^{7}Li+^{28}Si	8–350	1.3	21.046 (38.265)	1.245	0.657 (0.589)	120.493	0.948	0.632
^{9}Li+^{28}Si (see main body of the text)	18–500	1.3	22.532 (40.968)	1.245	0.667 (0.598)	120.493	0.948	0.632

$$\bar{V}(R)$$

$$V(R) = -V_0\left[1+\exp\left((R-R_V)/a_V\right)\right]^{-1} = \bar{V}(R)$$

$$W(R) = -W_0\left[1+\exp\left((R-R_W)/a_W\right)\right]^{-1}$$

Yu. E. Penionzhkevich *et al.*, Phys. Atom. Nucl., **80**, 928 (2017).

4.5. Energy-dependent nonadiabatic correction to the nuclear part of nucleus-nucleus potential

$$\mathrm{Re}\{V_{\mathrm{N}}(R)\} \equiv V(R, E_{\mathrm{lab}}) = \bar{V}(R) + \eta_2(E_{\mathrm{lab}})\boxed{\delta V_{\mathrm{d}}(R, E_{\mathrm{lab}})}$$ nonadiabatic correction

By analogy with a single folding potential

$$R = |\vec{r}_1 - \vec{r}_2|$$

$$\delta V_{\mathrm{d}}\left(R(t), E_{\mathrm{lab}}\right) = N \int_{\Omega} d^3 r \delta\rho_1(r,t) U_{\mathrm{T}}\left(|\vec{r} - \vec{r}_2(t)|\right)$$

Ω is the region of integration;

$$\delta\rho_1(r,t) = \rho_1(r,t) - \rho_1^{(0)}(r,t)$$

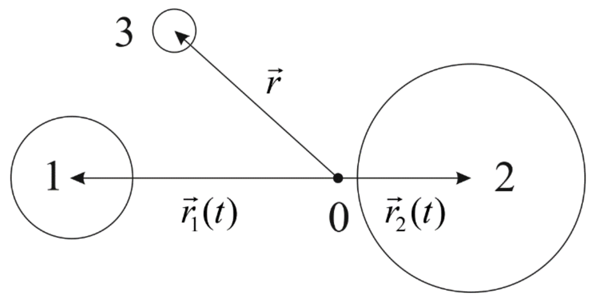

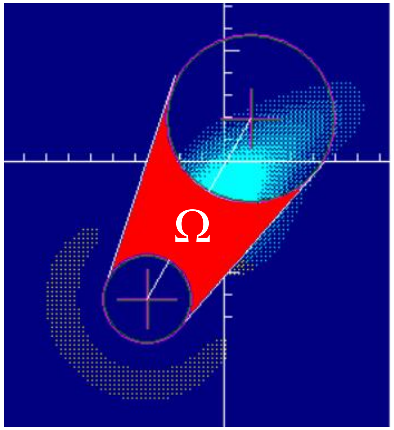

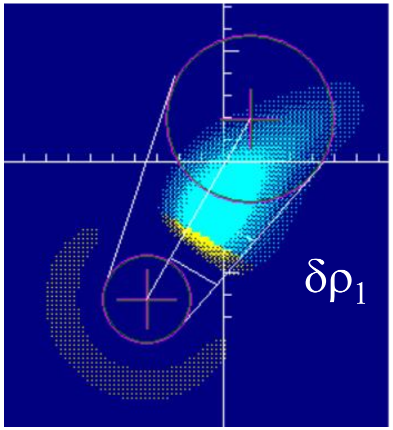

$\delta\rho_1(r,t)$ is change in the probability density due to rearrangement of neutrons between the projectile and the target;

$\rho_1(r,t)$ is the probability density of outer neutrons of the projectile nucleus taking into account their interaction with the target;

$\rho_1^{(0)}(r,t)$ is the probability density of outer neutrons of the projectile nucleus without taking into account their interaction with the target;

$U_{\mathrm{T}}\left(|\vec{r} - \vec{r}_2(t)|\right)$ is the mean field of the target nucleus for neutrons.

$N = 2$ is the number of independent neutrons for ^{9}Li (^{7}Li + n + n).

This way the effect of neutron rearrangement was taken into account

4.6. Potential of optical model depending on energy

$$\mathrm{Re}\{V_\mathrm{N}(R,E_\mathrm{lab})\} = \bar{V}(R) + \eta_2(E_\mathrm{lab})\delta V_\mathrm{d}(R,E_\mathrm{lab})$$

The change in the radius of the imaginary part was chosen proportional to change in the position of the real part (for example, as in [1]):

$$\mathrm{Im}\{V_\mathrm{N}(R,E_\mathrm{lab})\} = \begin{cases} -W_1, & R < R_b(E_\mathrm{lab}) \\ -W_1 \exp\left(-\dfrac{R-R_b(E_\mathrm{lab})}{b}\right), & R \geq R_b(E_\mathrm{lab}) \end{cases}$$

$$R_\mathrm{B}(E_\mathrm{lab}) = R_{\mathrm{B},0} + \delta R_\mathrm{B}(E_\mathrm{lab}),$$

$$R_b(E_\mathrm{lab}) = R_a + k\delta R_\mathrm{B}(E_\mathrm{lab}),$$

where R_a and k are parameters

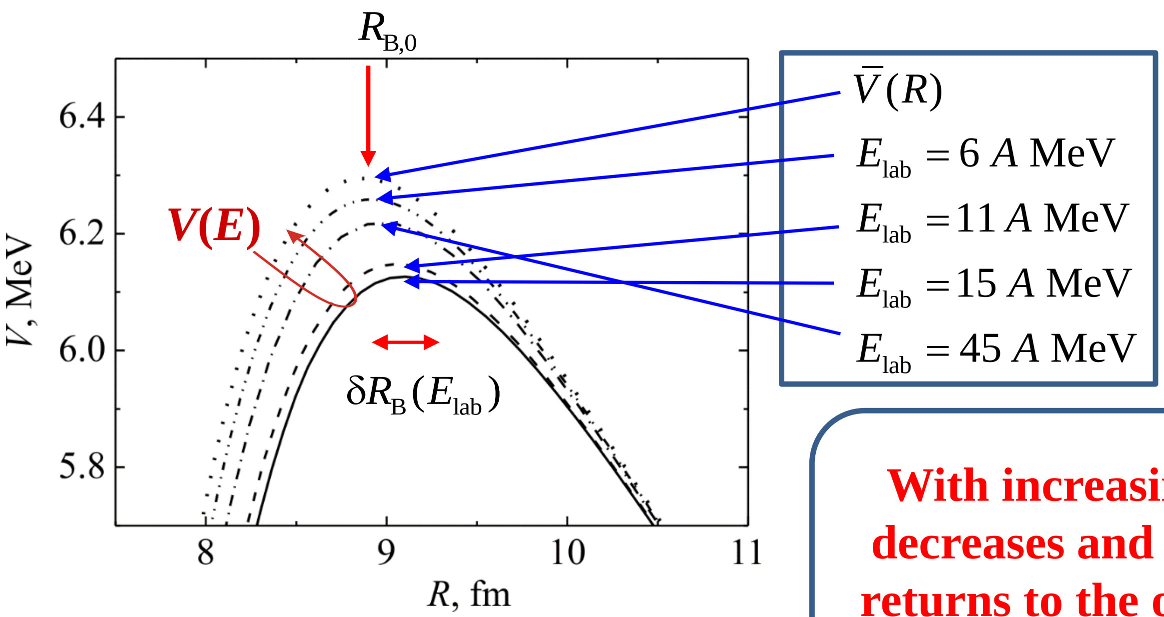

The change in the height and the position of the barrier with an increase of energy for ^{9}Li + ^{28}Si due to the rearrangement of neutrons [2].

With increasing energy, the barrier first decreases and shifts to the right, and then returns to the original energy-independent barrier

[1] Dymarz R. et al. // Z. Phys. A. **299,** 245. (1981).
[2] Yu. E. Penionzhkevich *et al*., Phys. Atom. Nucl., **80**, 928 (2017).

4.7. Total cross section and reaction probability due to interaction of ^{28}Si nucleus with ^{9}Li-like core of ^{11}Li nucleus

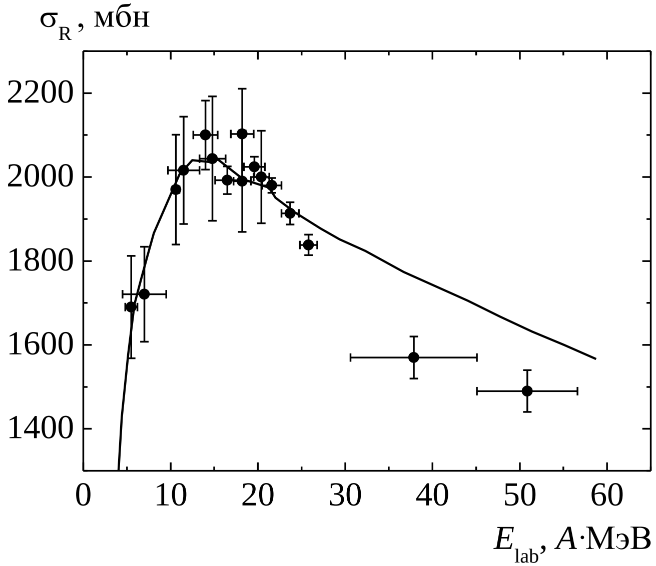

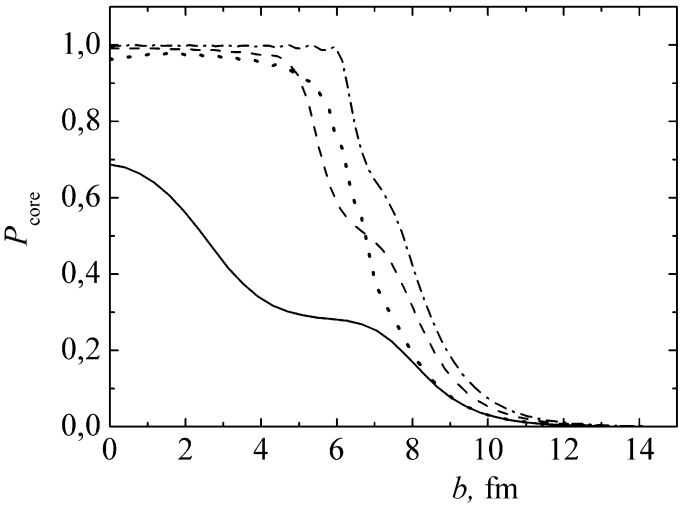

The total cross section for the reaction ^{9}Li + ^{28}Si: dots are experimental data, curve is the result of calculations in the optical model with an energy-dependent optical potential [1];

$$\sigma_R = \frac{\pi}{k^2}\sum_{l=0}^{\infty}(2l+1)\tilde{P}_{\mathrm{core}}(l,E)$$

quantum formula

$$l = kb$$

semiclasssical formula

$$\sigma_R = 2\pi\int_0^{\infty} P_{\mathrm{core}}(b,E)\,b\,db$$

The probabilities P_{core} of the reaction due to the interaction of the ^{28}Si nucleus with the ^{9}Li-like core of the ^{11}Li nucleus as a function of the impact parameter b for energies:
2.5 A MeV (solid line),
5 A MeV (dashed line),
12 A MeV (dot-dashed line),
50 A MeV (dotted line).

1. Yu. E. Penionzhkevich *et al.*, Phys. Atom. Nucl., **80**, 928 (2017).

4.8. Time-dependent microscopic description of dynamics of outer neutrons of ^{11}Li during collision ^{11}Li + ^{28}Si

^{11}Li was represented as core ^{9}Li + *n* + *n*

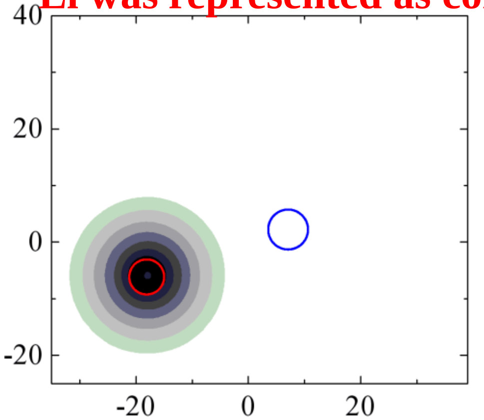

E_{lab}= 12.6 *A* MeV

E_{lab}= 50 *A* MeV

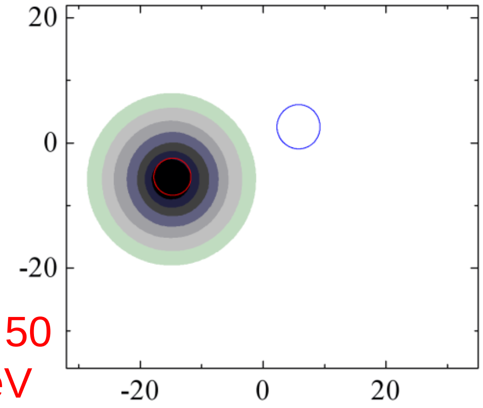

fm

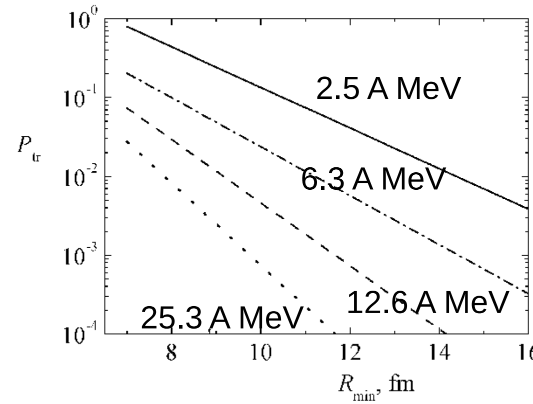

The probabilities of neutron transfer to unoccupied bound states of discrete spectrum of the ^{28}Si

Animation:

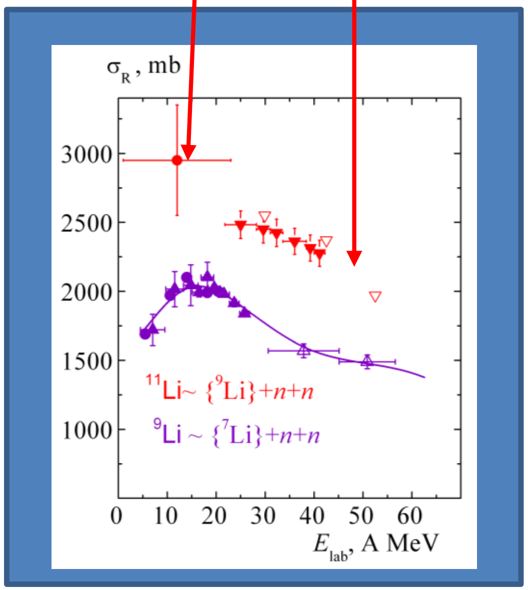

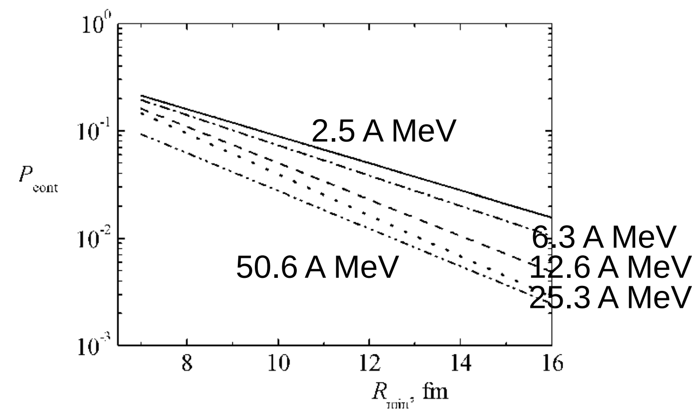

An example of evolution of the probability density $\rho(\mathbf{r},t)$ of external neutrons of the ^{11}Li nucleus in its collision with the ^{28}Si nucleus at energy E_{lab}= 12.6 A MeV (E_{cm}=100 MeV) (a) and E_{lab}= 50.6 A MeV (E_{cm}=400 MeV) (b)

The probabilities of neutron transfer to states of continuous spectrum

4.9. The total cross section σ_R for the reaction ^{11}Li + ^{28}Si

^{11}Li was represented as core ^{9}Li + *n* + *n*

$$\sigma_R = 2\pi \int_0^\infty P_R(b,E)\,b\,db \qquad (1)$$

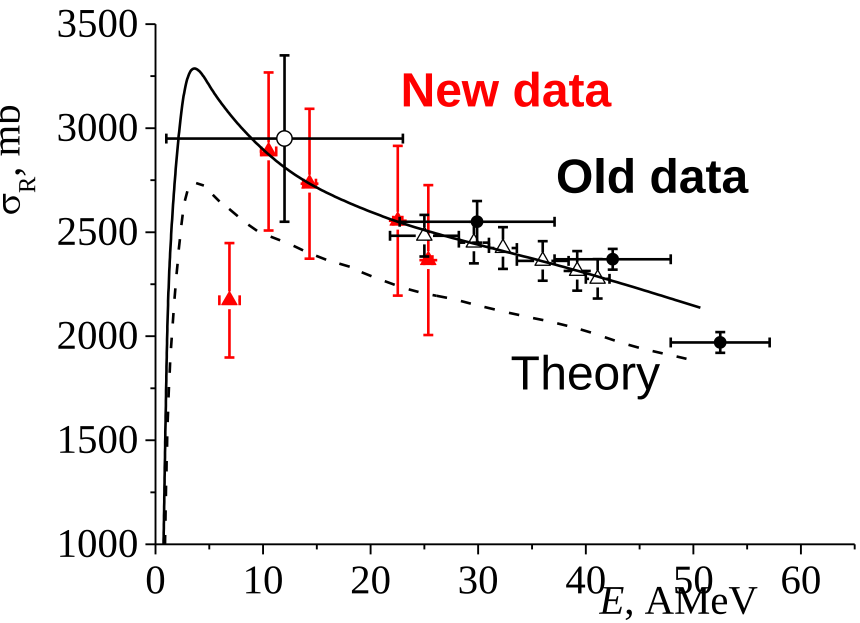

Experimental (symbols) and calculation for C = 1 (dashed curve) and C = 2 (solid curve) for the total reaction cross section ^{11}Li + ^{28}Si: solid (red) triangles are the new results of [4]. Other data for ^{11}Li: filled circles [3], empty circle [1], empty triangles [2].

The probability of reaction

$$P_R(b,E) = 1 - \left[1 - P_{\text{core}}(b,E)\right]\left[1 - P_{\text{loss}}(b,E)\right]^2 \qquad (2)$$

P_{core} is the probability of the reaction due to the interaction of the ^{28}Si nucleus with the ^{9}Li-like core

The probability of neutron loss (removal) from ^{11}Li

$$P_{\text{loss}}(b,E) = \min\left\{P_{\text{tr}}(b,E) + P_{\text{cont}}(b,E), 1\right\} \qquad (3)$$

The probabilities of neutron transfer to unoccupied bound states (of discrete spectrum) of the ^{28}Si

$$P_{\text{tr}}(b,E) = \lim_{t\to\infty} \sum_{\substack{k \\ \varepsilon_k > E_F}} \left|a_k(t)\right|^2 \qquad (4)$$

The probabilities of neutron transfer to states of continuous spectrum

$$P_{\text{cont}} = C \max\left\{\int_D \rho(\mathbf{r},t)\,d\mathbf{r}\right\} \qquad (5)$$

The total cross section for the reaction ^{11}Li + ^{28}Si: symbols are experimental data [1-3], curves are the results of the calculation for the values of the adjustable parameter $C = 1$ (dashed line) and $C = 2$ (solid line) with the probability P_{cont} of transfer to the states of continuous spectrum calculated by formula (5)

[1] A.C. Villari *et al.,* Phys. Lett. B **268**, 345 (1991). [2] LI Chen *et al.,* High Energy Physics and Nuclear Physics **31**, 1102 (2007).
[3] R.E. Warner *et al*., Phys. Rev. C **54**, 1700 (1996). [4] Yu. E. Penionzhkevich *et al*., NUCLEUS2018, Voronezh

5.1. Animation: probability density of outer neutrons for head-on collision ^{40}Ca+^{96}Zr at $E_{c.m.}$=98 MeV and of two-center (2C) states [1]

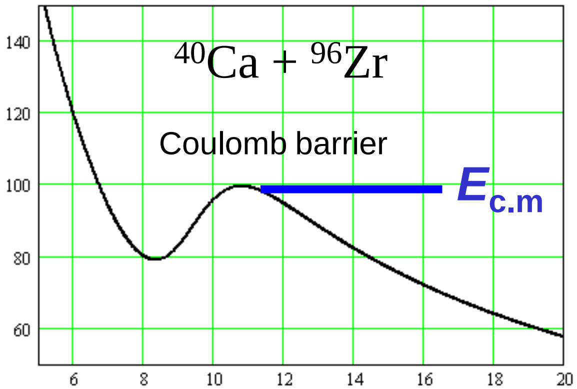

interaction potential for nuclei ^{40}Ca and ^{96}Zr

$2d^{6}_{5/2}(^{96}\mathrm{Zr})$

2C-states:

Ω=1/2

$1f_{7/2}$(Ca)

$1g_{9/2}$(Zr)

$2p_{3/2}$(Ca)

$2d_{5/2}$(Zr)

$3s_{1/2}$(Ca)

$1g_{7/2}$(Zr)

Ω=3/2

$1f_{7/2}$(Ca)

$1g_{9/2}$(Zr)

$2p_{3/2}$(Ca)

$2d_{5/2}$(Zr)

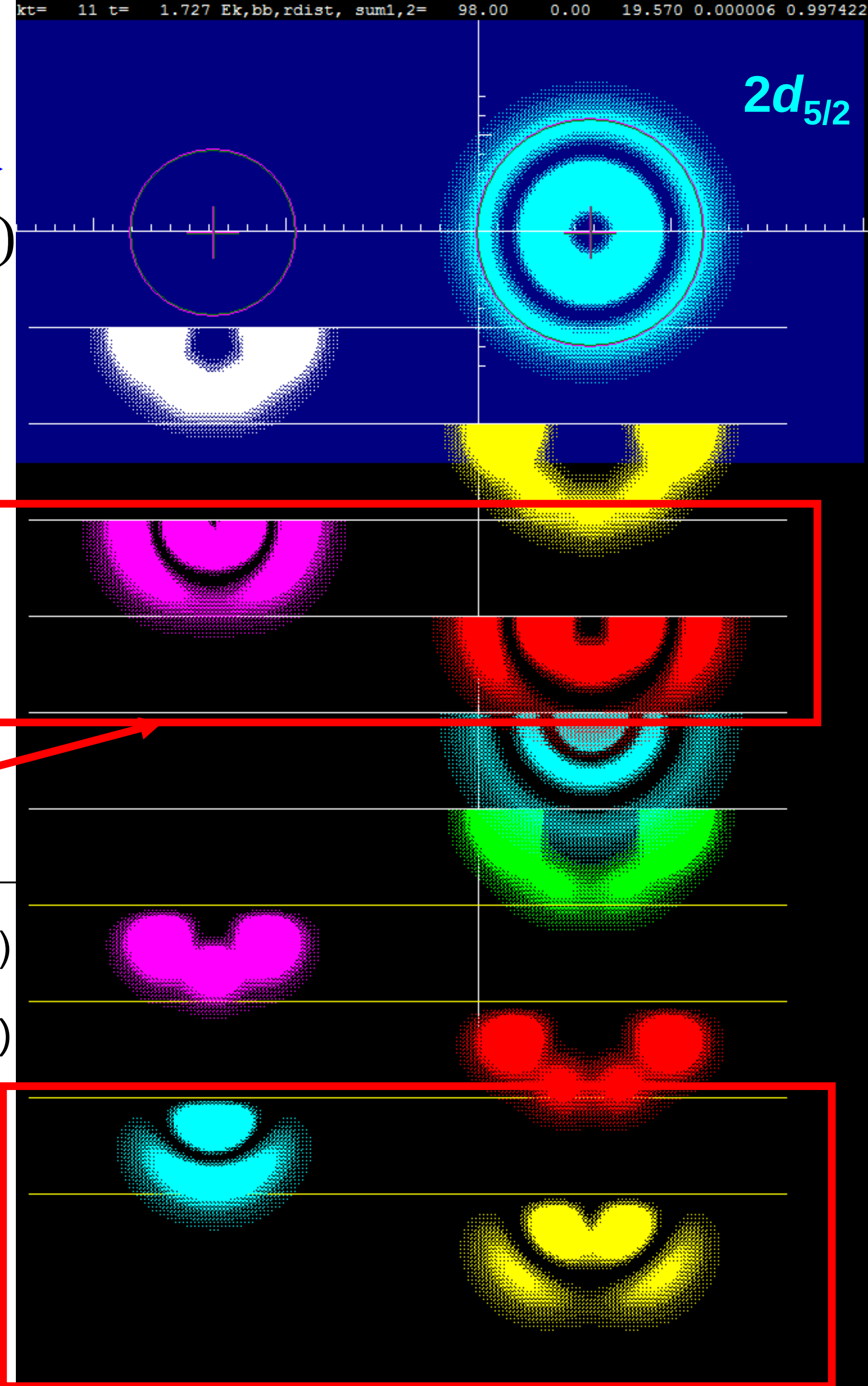

These 2C-wave functions are overlapping strongly.
Most probable transition is $2d_{5/2}(^{96}$Zr) to $2p_{3/2}(^{40}$Ca)

Ω is absolute value of the total-angular-momentum projection onto the nucleus-nucleus axis

Calculation method:

[1] V. Samarin. Phys. Atom. Nucl. **78**, 128 (2015).

5.2. Neutron levels in shell model of ^{40}Ca, ^{90}Zr and system ^{40}Ca + ^{90}Zr

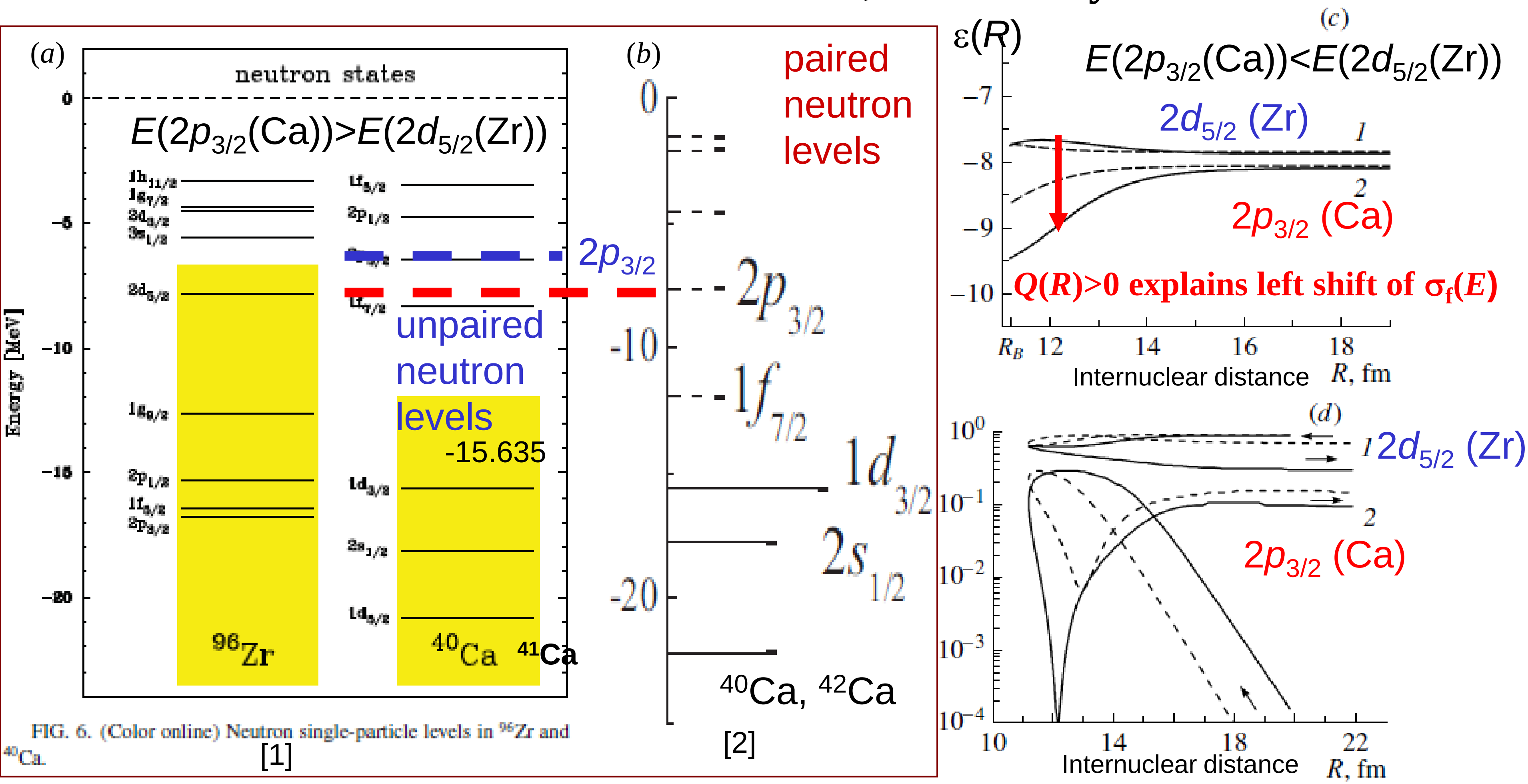

[1]. L. Corradi et al., Phys. Rev. C **84**, 034603 (2011).

(c) Energies of those neutron two-center levels for the absolute values Ω=1/2 (solid curves) and Ω=3/2 (dashed curves) of the total-angular-momentum projection onto the nucleus-nucleus axis (z axis) in the ^{40}Ca+^{96}Zr system that correspond to the (curve 1) $2d_{5/2}$ state of ^{96}Zr nucleus and (curve 2) $2p_{3/2}$ state of ^{40}Ca nucleus;
(d) occupation probabilities for the corresponding two-center states in head-on ^{40}Ca+^{96}Zr collision at $E_{\mathrm{c.m.}}$=98 MeV [2]

[2]. V. Samarin. Phys. Atom. Nucl. **78**, 128 (2015).

5.3. Rearrangement of neutrons and initial stage of fusion

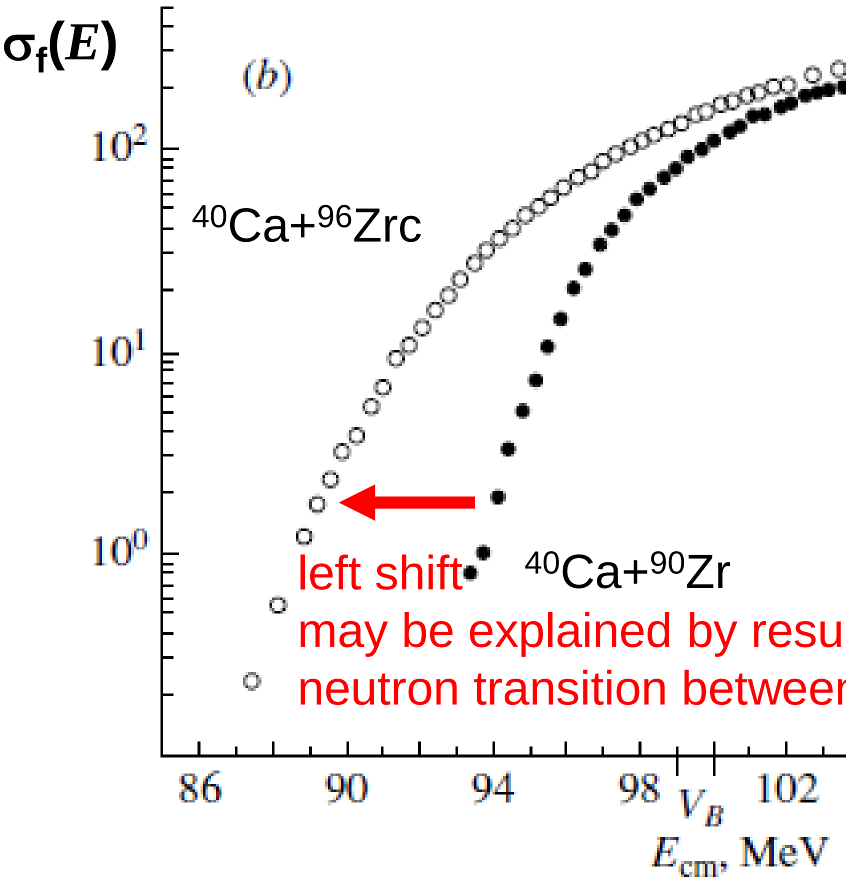

probability density of outer neutrons

these 2C-wave functions are overlapping strongly. Most probable transition is $2d_{5/2}$(^{96}Zr) to $2p_{3/2}$(^{40}Ca)

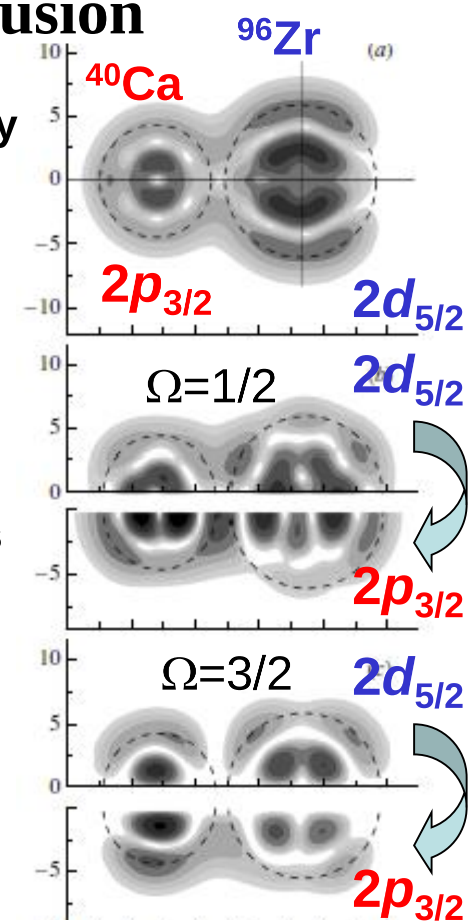

Fig. 5. (a) Probability density for neutrons of the $2d^6_{5/2}$ outer shell in the ^{96}Zr nucleus (right-hand object) near the turning point in a central collision with a ^{40}Ca nucleus (left-hand object) at $E_{\rm c.m.} = 98$ MeV; (b and c) probability densities for the two-center states corresponding to the $2d_{5/2}$ state of the ^{96}Zr nucleus (upper part) and the $2p_{3/2}$ state of the ^{40}Ca nucleus (lower part) for the following absolute values of the total-angular-momentum projection onto the nucleus–nucleus axis (z axis): $\Omega = 1/2$ (b) and $\Omega = 3/2$ (c).

Experimental data on the cross sections for fusion of nuclei in the reactions ^{40}Ca+^{96}Zr (empty circles) and ^{40}Ca+^{90}Zr (filled circles). Here V_B stands for the Coulomb barrier [1].

[1] M. Trotta et al., Phys. Rev. C **65**, 011601(R) (2001).

5.4. Rearrangement of neutrons and initial stage of fusion

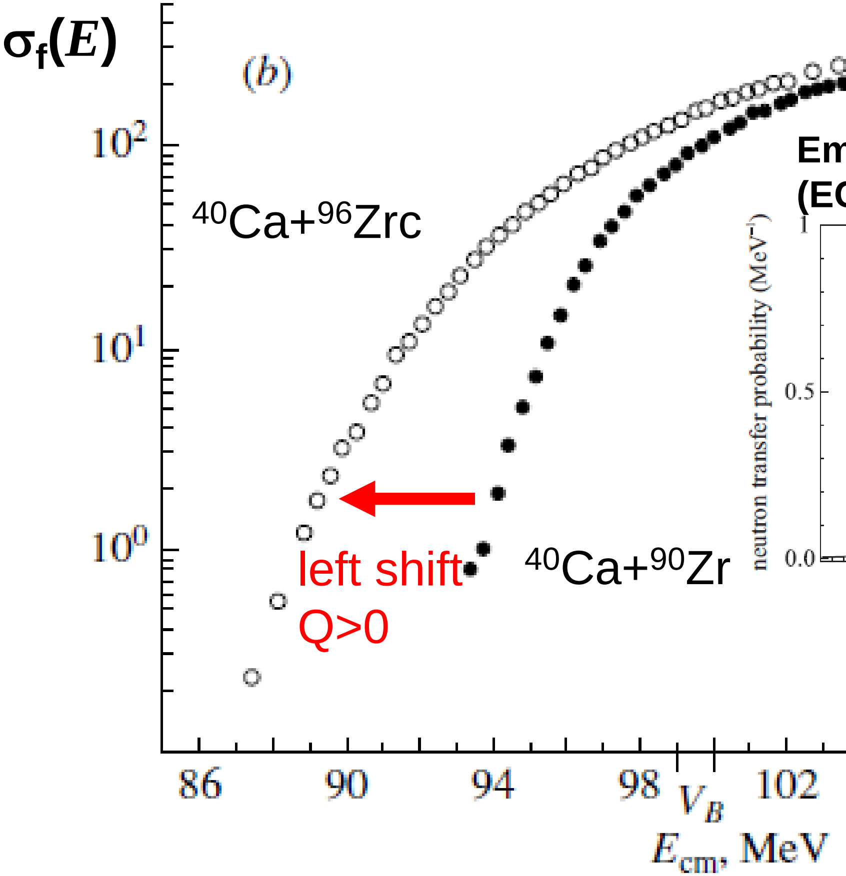

Experimental data on the cross sections for fusion of nuclei in the reactions ^{40}Ca+^{96}Zr (empty circles) and ^{40}Ca+^{90}Zr (filled circles). Here V_B stands for the Coulomb barrier [1].

[1] M. Trotta et al., Phys. Rev. C **65**, 011601(R) (2001).

Empirical coupled-channel (ECC) model [2]

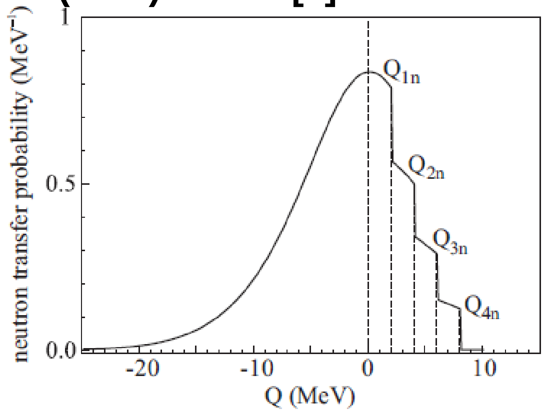

Typical behavior of empirical neutron transfer probability as function of Q-value in ENR model [2,3]

Quantum coupled channel + empirical neutron rearrangement (QCC+ENR) model [3]

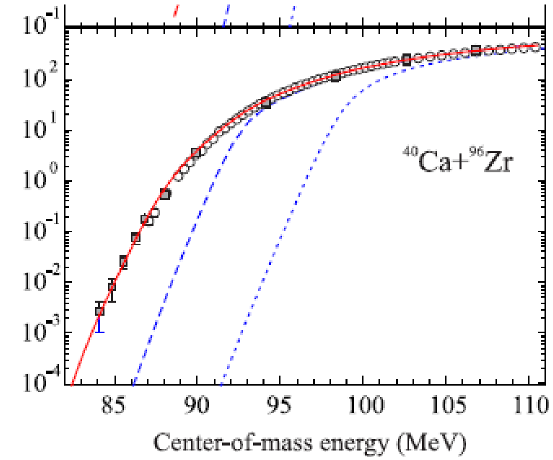

Fusion cross section for ^{40}Ca+^{96}Zr. The dotted curves show the no-coupling limit. The solid and dashed curves correspond to the calculation with (QCC+ENR model) and without (QCC model) taking into account neutron transfer, respectively [3].

[2] V.I. Zagrebaev, Phys. Rev. C **67**, 061601 (2003).
[3] A.V. Karpov, V.A. Rachkov, V.V. Samarin, Phys. Rev. C, **92**, 064603 (2015)

TDSE is the microscopic validation of empirical neutron rearrangement (ENR) and empirical coupled-channel (ECC) models.

5.5. Nucleons rearrangement in reaction $^{40}Ca+^{124}Sn$

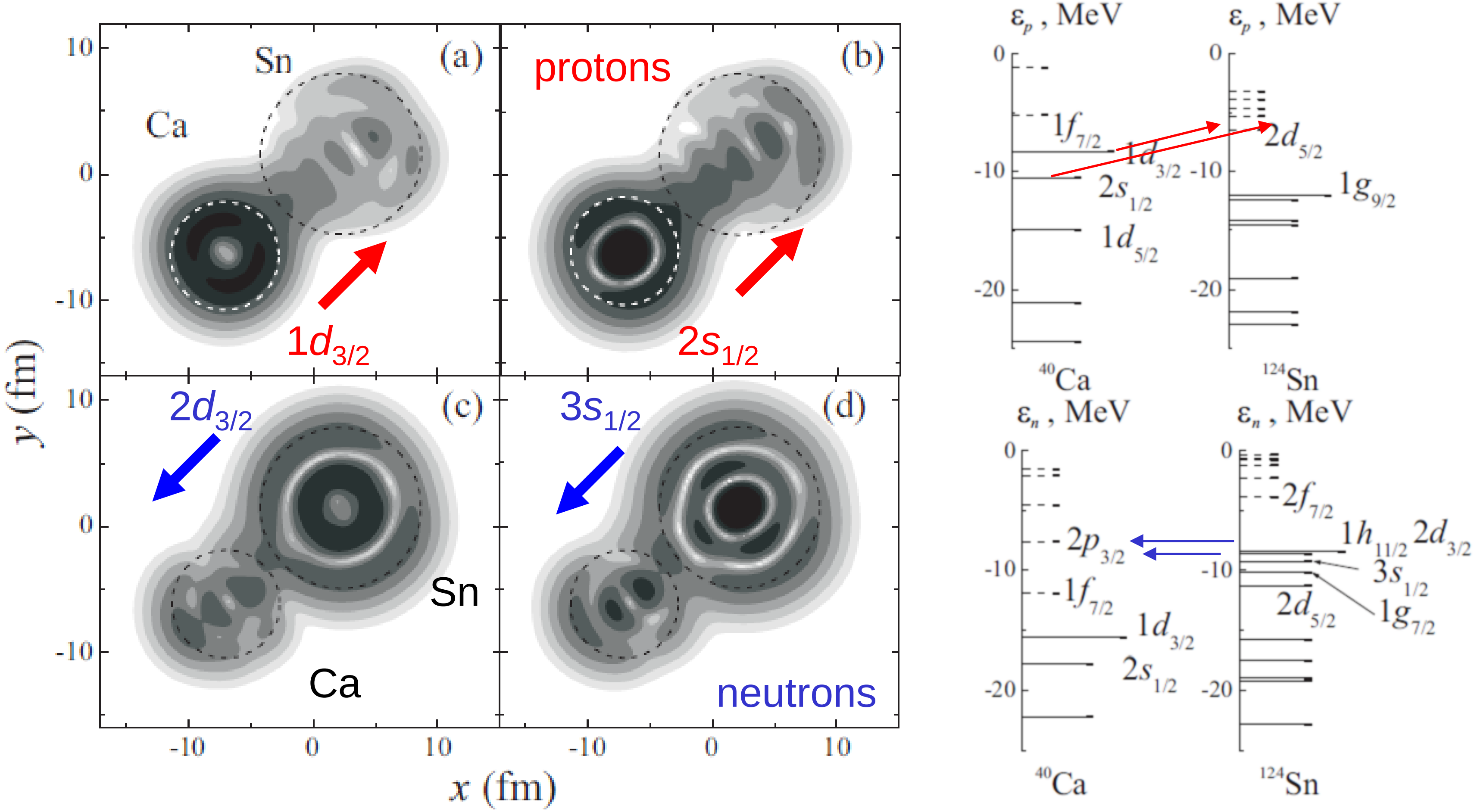

The probability density for the protons of the ^{40}Ca nucleus with the initial states $1d_{3/2}$ (a) and $2s_{1/2}$ (b) and the probability density for the neutrons of the ^{124}Sn nucleus with the initial states $2d_{3/2}$ (c) and $3s_{1/2}$ (d) at the closest approach of nuclei ^{40}Ca and ^{124}Sn in the collision with the energy in the center-of-mass system 128 MeV and the impact parameter 4 fm. The distance between the centers of the nuclei is 12 fm, the radii of the circles are equal to the radii of the nuclei.

5.6. Nucleon rearrangement and multineutron transfer in reaction $^{40}Ca+^{124}Sn$

In the ^{40}Ca nucleus, there are six filled proton and neutron shells and in the ^{124}Sn nucleus 11 proton shells and 16 neutron shells are filled.

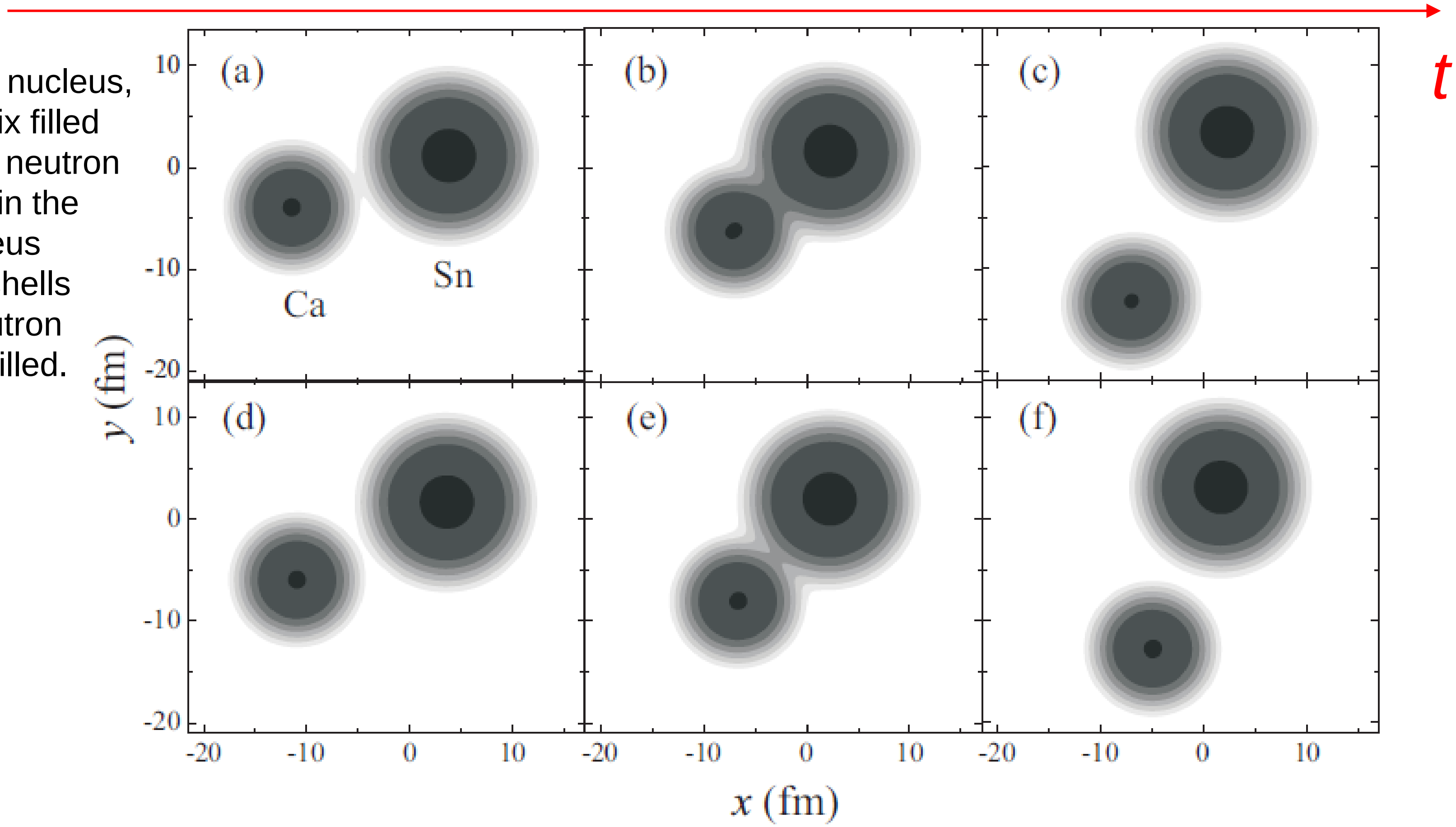

Evolution of the probability density of all nucleons of the nuclei ^{40}Ca and ^{124}Sn in collision with the energy in the center-of-mass system 128 MeV and the impact parameter 4 fm (a, b, c) and 6 fm (d, e, f). The course of time corresponds to the panel locations (a, b, c) and (d, e, f).

5.7. Proton stripping and neutron pick-up in reaction ^{40}Ca + ^{124}Sn

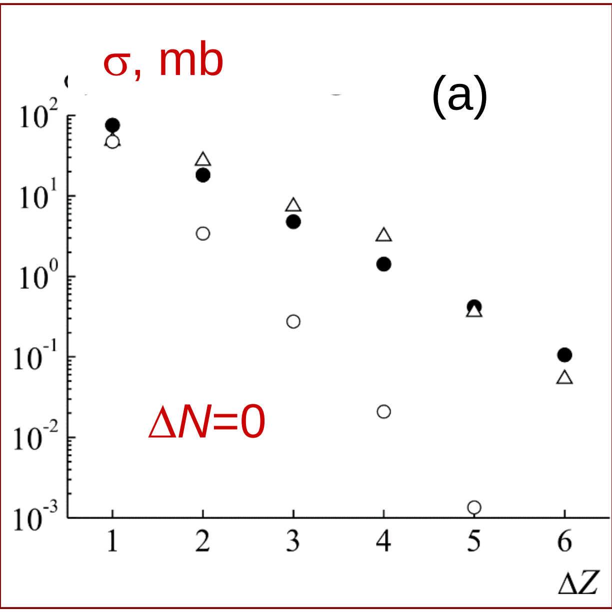

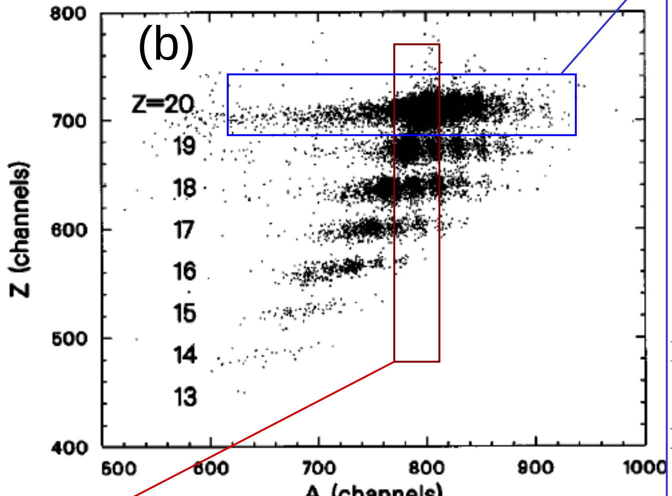

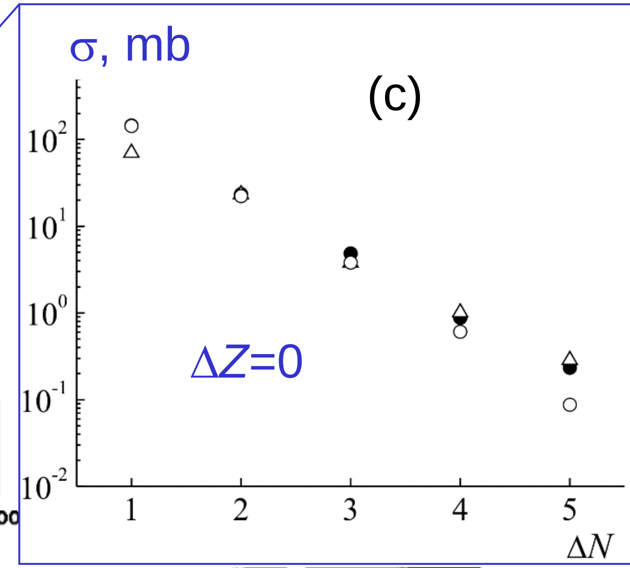

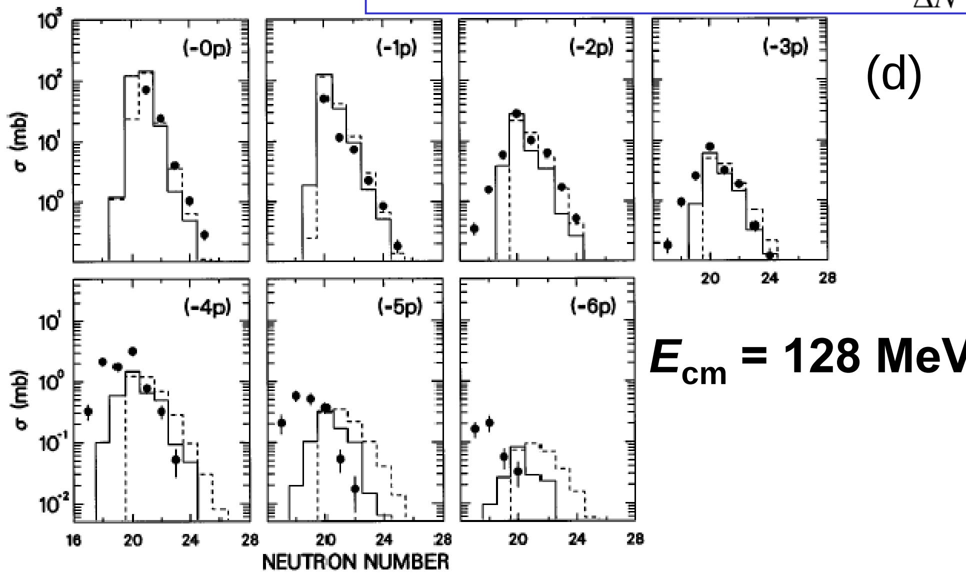

(a) The cross sections for reactions involving stripping of Δ*Z* protons without neutron transfer (Δ*N*=0);
(c) the cross sections for reactions with proton pickup without neutron transfer (Δ*Z*=0); triangles are experimental data from Ref. [1]; dots are the calculations of this work; circles are calculations using the code GRAZING [2,3];
(b), (d) experimental data from Ref. [1].

FIG. 3. Experimental (points) and calculated (histograms) total integrated cross sections for the transfer products. Expe take into account statistics and systematic errors coming from monitor and spectrometer solid angle determination, beam foc tion of the mass and charge spectra, and integration of the angular distributions. The dashed lines represent the cross section yields; this has been shown to illustrate the importance of neutron evaporation.

[1]. L. Corradi et al., Phys. Rev. C **54**, 201 (1996).
[2]. NRV web knowledge base on low-energy nuclear physics. http://nrv.jinr.ru/
[3].http://personalpages.to.infn.it/~nanni/grazing/

Conclusions

- The numerical solution of the time-dependent Schrödinger equation is applied to analysis of dynamics of nucleon transfer and rearrangement at energies near and above the Coulomb barrier.
- The evolution of wave functions of all nucleons is used for the description of neutron and proton transfer in reactions $^{3,6}He + ^{197}Au$, $^{3}He + ^{194}Pt$, $^{3,6}He + ^{45}Sc$, $^{9}Li + ^{28}Si$, $^{40}Ca+^{124}Sn$ and total cross sections of reactions $^{11}Li + ^{28}Si$. The results of calculations of transfer cross sections are in satisfactory agreement with experimental data.
- The evolution of wave functions of outer neutrons is used for the microscopic validation of empirical neutron rearrangement (ENR) and empirical coupled-channel (ECC) models and explanation of energy dependence of fusion cross section for reaction $^{40}Ca+^{96}Zr$.

Acknowledgments

This work was supported by the Russian Science Foundation (RSF), research project No. 17-12-01170.

RSF | Russian Science Foundation

Thank You